IODINE DYNAMICS IN SOILS

SHETAYA W.H.[1,2], YOUNG S.D.[1], WATTS M.J.[3], ANDER E.L.[3] & BAILEY E.H.[1,*]

[1]Division of Agriculture and Environmental Science, School of Biosciences, University of Nottingham, Sutton Bonington, Leicestershire LE12 5RD
[2]Environmental Sciences Division, National Research Centre, El-Tahrir St, Dokki, Cairo (12311), Egypt
[3]British Geological Survey, Nicker Hill, Keyworth, Nottingham, NG12 5GG
*Corresponding Author, Tel: +44 (0)115 951 6255, E-mail: liz.bailey@nottingham.ac.uk

1. ABSTRACT

We investigated changes in iodine (^{129}I) solubility and speciation in nine soils with contrasting properties (pH, Fe/Mn oxides, organic carbon and iodine contents), incubated for nine months at 10°C and 20°C. Loss of I^- from solution was extremely rapid, apparently reaching completion over minutes-hours; IO_3^- loss from solution was slower, typically occurring over time periods of hours-days. For both I^- and IO_3^- losses were faster in soils with greater soil organic carbon contents (%SOC) and low pH and at higher temperatures (10°C cf. 20°C). Instantaneous sorption of IO_3^- was identified in all soils and was greatest in a soil with high Fe/Mn oxide, low pH and low SOC content. Evidence for immediate sorption of I^- was less clear as reaction rates were faster. Phosphate extraction (0.15 M KH_2PO_4) of soils, ~100 hr after ^{129}I spike addition, indicated that concentrations of sorbed inorganic iodine (^{129}I) were very low in all soils suggesting that, even if IO_3^- is initially adsorbed onto oxide phases, this has little impact on the rate of iodine assimilation into humus.

The transformation of dissolved inorganic $^{129}IO_3^-$ and $^{129}I^-$ to sorbed organic forms was modelled using a range of reaction- and diffusion-based approaches. Irreversible and reversible first order kinetic models, and a spherical diffusion model, adequately described the kinetics of both IO_3^- and I^- loss from the soil solution but only with the inclusion of a distribution coefficient term (kd) to allow for instantaneous adsorption. The spherical diffusion model produced the lowest average RSD value for IO_3^- sorption by all soils and all three models gave almost identical average RSD values in the case of I^-. A spherical diffusion model was collectively parameterised for all the soils by using pH, soil organic carbon concentration and combined Fe+Mn oxide content as determinants of the model parameters (kd and D/r^2). From the temperature-dependence of the sorption data the activation energy (Ea) for $^{129}IO_3^-$ transformation to organic forms was estimated to be ~43 kJ mol^{-1}. The Ea value was independent of %SOC and suggests a reaction mechanism that is slower than pore diffusion or physical adsorption but faster than most surface reactions.

2. INTRODUCTION

Iodine is an essential trace element for human and animal health. It is used by the thyroid gland in the production of hormones which control a range of physiological processes. Insufficient thyroid hormone levels are associated with a range of health issues including problems of growth and development in children, and goitre in adults (Trotter, 1960; Underwood, 1977). Collectively, iodine deficiency diseases (IDDs) are a serious worldwide health problem, estimated to affect ~35% of the world's population, and a significant social and economic stress on developing countries (WHO, 2004).

Rocks contain little iodine and most soil iodine is derived from volatilization of methylated forms from seawater which then enter the soil-plant system via rainfall and dry deposition. IDDs are prevalent in regions where people have limited access to food that is naturally rich in iodine (e.g. seafood) or iodized food products (Underwood, 1977; Johnson et al., 2002). Availability of iodine in such regions depends largely on transfer from soil to food or fodder crops but local produce may not be able to supply the recommended daily intake of dietary iodine (Johnson, 2003). There is therefore a need to increase our knowledge of iodine behaviour in soil, in particular how added iodine (in rainfall or fertilizers) reacts with soil and the mechanisms by which iodine becomes available to plants. Furthermore, understanding the environmental behaviour of long lived iodine isotopes (^{129}I $t_{½}$ = 1.6 x 10^7 y) is also essential to the safety case for underground nuclear waste disposal; ingestion of radioiodine released from weapons testing, nuclear power stations, medical or research facilities may induce thyroid tumours or supress thyroid function (Furhmann et al., 1998; Bonhoure et al., 2002).

Iodine is found in nature in several valence states and in a range of inorganic and organic forms including iodide (I^-), iodate (IO_3^-), elemental iodine (I_2) and organic iodine (Radlinger and Heumann, 1997; Schwehr and Santschi, 2003; Muramatsu et al., 2004; Gilfedder et al., 2007a,b; Liu et al., 2007; Yang et al., 2007; Yoshida et al., 2007). Its form depends on pH and the redox status of the surrounding environment; thus iodide is reported as the most prevalent form of iodine in river waters while iodate is most common in the oceans (Smith and Butler, 1979; Abdel-Moati, 1999). In rainwater a mix of species including iodate, iodide and organic iodine species have been reported (Gilfedder et al., 2008). Inorganic iodine forms may be retained in acidic soils by sorption on positively charged hydrous iron and aluminium oxides (Whitehead, 1974a) and possibly up

to pH 8 by specific adsorption of iodate (Yoshida et al., 1992). However, strong assimilation of iodine into soil organic matter has been widely reported (e.g. Whitehead, 1973a; Francois, 1987a&b; Fukui et al., 1996; Sheppard et al., 1996; Yu et al., 1996; Steinberg et al., 2008a&c; Dai et al., 2009) and humus may constitute the primary reservoir of iodine in most soils. The fate of inorganic iodine, and the mechanisms governing its incorporation into organic matter, have been the focus of a number of investigations. Reduction of iodate by soil organic matter may precede conversion of inorganic iodine into organic forms (Whitehead, 1974b, Fukui et al., 1996). Steinberg et al. (2008b) confirmed that iodate heated with peat and lignin over a pH range of 3.5-9 was converted to organic iodine forms and iodide; Francois (1987a) observed that the iodine content of humic substances increased following incubation with iodate for 5 days. In both cases it was shown that iodate was first reduced to reactive intermediate products, I_2 or HOI, which then reacted rapidly with the organic matter. From a study of reaction kinetics, Warner et al., (2000) concluded that iodination of natural organic matter followed the same mechanism as iodination of phenols, through reaction with molecular iodine, I_2. The same electrophilic substitution mechanism was suggested by Reiller et al., (2006) in their study of iodination of humic acids. Bichsel and von Gunten (1999, 2000) also demonstrated that iodide can be oxidised to HOI and thereby react with organic compounds (e.g. substituted phenol and methyl carbonyl compounds) similar to natural humic matter. Yamaguchi et al. (2010) observed that iodine K-edge XANES spectra of soils spiked with iodide and iodate were similar to organic iodine standard spectra after 60 days incubation. They also found that iodide was fully transformed into organic forms after 1 day of incubation in highly organic soils, and was fully transformed in all soils after 60 days. By contrast, no measureable iodate transformation was observed after 1 day of incubation and up to 50% of the added iodate remained in the lower organic matter soils at 60 days. A comparison of iodine L_{III}-Edge XANES and EXAFS spectra of iodinated organic compounds with naturally iodated humic substances, extracted from a range of soil types, indicated that organic iodine is primarily bonded to aromatic rings (Schlegel et al., 2006).

Metal oxides and hydroxides (eg $Fe^{III}(OH)_3$, $Al(OH)_3$, $Mn^{IV}O_2$) may play an important role in controlling iodine behavior in soils, both through adsorption of inorganic iodine and oxidation of iodide. Ferric and aluminium oxides adsorb iodate more strongly than iodide (e.g. Whitehead, 1974a; Kodama et al., 2006). Oxidation of I^- to I_2 and then to IO_3^- has been shown to be catalysed by δ-MnO_2 with IO_3^- adsorbing on the δ-MnO_2 surface

(Gallard et al., 2009). In the presence of humic substances the oxidation to IO_3^- is limited as I_2 can react to form organic iodine (org-I) species, especially at lower pH (Gallard et al., 2009).

In view of the importance of iodine sorption by soils in regulating plant bio-availability and losses to drainage water and also considering the current lack of information regarding which soil factors govern reaction mechanisms and rates, the aims of this investigation were to:

(i) measure the dynamics of iodide and iodate (^{129}I) transformation in soils, both in the solution and solid phases, in order to increase our understanding of the reaction process and rate;

(ii) account for the effects of soil factors likely to influence the adsorption and transformation of iodine species, including temperature, pH value and concentrations of soil organic carbon (SOC), Fe/Mn oxides and native iodine.

(iii) integrate the data from ^{129}I incubation experiments into a predictive model of iodate and iodide sorption kinetics parameterized by soil properties.

3. MATERIALS AND METHODS

3.1 Soil sampling and preparation

Topsoil and subsoil were sampled from two areas in the East Midlands of England, chosen to represent contrasting land-uses, soil pH values and concentrations of Fe/Mn oxides, organic matter, carbonate and iodine. Wick series (sandy loam) soil samples were taken from an arable field, a permanent grassland strip and adjacent mature deciduous woodland (Grid Reference 52°49'48"N-1°14'88"W) on the University of Nottingham farm, Sutton Bonington, Leicestershire (UK). Topsoil (0-20 cm depth) and subsoil (30-50 cm depth) samples were taken from the arable and woodland sites; only topsoil was sampled from the grassland as its associated subsoil was thought to be similar to the arable subsoil. Iodine concentrations in these soils were known to be low (2 - 4 mg kg^{-1}) from previous analysis. Soils with higher iodine concentrations (c. 8 – 12 mg kg^{-1}, Johnson et al., 2005) were sampled on the Stoke Rochford Estate, Lincolnshire from the Elmton soil series, described as shallow, well-drained brashy calcareous fine loamy soils developed over Jurassic limestone. Grassland and woodland topsoils (0-20 cm) were collected from a valley with permanent grassland (52°50'53"N-0°40'26"W) and adjacent mature woodland (52°50'56"N-0°40'22"W); these are Lithomorphic Rendzina soils over limestone and thus have no associated subsoil. Arable topsoil (0-20 cm) and subsoil (30-50 cm) samples were taken from a field nearby (52°51'25"N-0°38'55"W). Samples were collected with clean stainless steel spades, augers and trowels and sealed in plastic bags for transport. Soils were air dried until they could be sieved to <4 mm but were not allowed to dry completely so as to maintain microbial activity; they were then kept unsealed in a cold room (at 10°C) prior to use, to ensure they remained aerobic and to preserve remaining moisture content.

3.2 Soil chemical properties

Approximately 250 g of each soil was air dried and sieved (< 2 mm) for analysis. Soil pH was measured using a combined glass electrode after equilibrating 5 g of soil in 12.5 mL of Milli-Q water (18.3 MΩ) for 30 minutes. Carbonate content of soils was estimated by manometric assay using a Collins calcimeter (Piper, 1954). Loss on ignition (LOI) was determined gravimetrically after heating soil (c. 5 g) in a muffle furnace at 550°C for 16 hours. Organic carbon content was determined (Elementar VarioMax CN analyser) on samples of finely ground soil (agate ball mill, Retsch Model PM400) after acidification with HCl (50% v/v) to remove inorganic carbon. The limit of quantification reported for a typical 300 mg sample is 0.18%. The dithionite extraction method of

Kostka and Luther (1994) was used to determine reactive iron, aluminium, and manganese hydrous oxides; after reaction samples were centrifuged (20 min at 3000 g), filtered (<0.22 μm) and supernatant solutions retained for analysis. Total soil iodine was extracted with tetra methyl ammonium hydroxide (TMAH) from finely ground soil samples according to the method developed by Watts and Mitchell (2009).

Elemental concentrations were assayed using a Thermo-Fisher Scientific X-Series^{II} ICP-MS in standard mode (for iodine) and employing a 'hexapole collision cell' (7% H_2 in He) prior to the analytical quadrupole for Fe, Al, and Mn analysis. Samples were introduced from an autosampler (Cetac ASX-520 with 4 x 60-place sample racks) through a concentric glass venturi nebuliser (Thermo-Fisher Scientific; 1 mL min^{-1}) and Peltier-cooled spray chamber (3^{o}C). Internal standards were introduced to the sample stream via a T-piece and included 20 ng mL^{-1} In, 20 μg L^{-1} Re, and 20 μg L^{-1} Rh, prepared in a matrix of 2% TMAH and 4% methanol for iodine analysis and Sc (100 μg L^{-1}), Rh (20 μg L^{-1}) and Ir (10 μg L^{-1}) in 2% 'trace analysis grade' (TAG) HNO_3 for Fe, Al and Mn. An iodine stock standard (1000 mg ^{127}I L^{-1}) was prepared from oven-dried analytical grade KI in a matrix of 5% TMAH and stored at 4^{o}C; dilutions of this stock were used for instrument calibration. Multi-element calibration standards (Claritas-PPT grade CLMS-2, Certiprep/Fisher), including Fe, Al and Mn, were all diluted in 2% Trace Analysis Grade HNO_3 in the range 0-100 μg L^{-1}. Sample processing was undertaken using Plasmalab software (version 2.5.4; Thermo-Fisher Scientific) using internal cross-calibration where required. Limits of detection (LOD) were calculated from analysis of 16 blanks (3 x standard deviation of blanks) to be 1.26 μg L^{-1} (~0.008 mg kg^{-1}) for ^{127}I and 0.34 μg L^{-1} (~ 0.002 mg kg^{-1}) for ^{129}I.

3.3 Soil Incubation

Samples of ^{129}I, as sodium iodide solution (SRM 4949C, 0.004 mol L^{-1} $Na^{129}I$, 3451 Bq mL^{-1}), were obtained from the American National Institute of Standards (NIST), Gaithersburg, Maryland, USA. Iodate ($^{129}IO_3^-$) was prepared from $^{129}I^-$ by oxidation using sodium chlorite as described by Yntema and Fleming, (1939). Soil samples for incubation were prepared by mixing moist sieved soil (< 4 mm) in a food mixer with Milli-Q water (controls) or an equivalent volume of $^{129}I^-$ or $^{129}IO_3^-$ solution to give a final ^{129}I concentration of 0.15 mg kg^{-1} (in dry soil). The water content of the incubated soil is inevitably an arbitrary choice. The total volume of solution added to each soil was simply judged from the friability of the aggregated soil rather than being based on a fixed proportion of water holding capacity or a specific soil moisture tension. We considered the need to

maintain moist but aerobic soils capable of free gas exchange and able to be sub-sampled for periodic analysis; the final water contents of the incubated soils are shown in Table 1. Spiked soils were distributed between triplicate 500 mL Duran bottles (~180 g dry wt of soil per replicate) with a hole drilled in the lid to allow gas exchange, and incubated in the dark at 10°C or 20°C (± 2°C). Moisture loss was monitored regularly and restored when necessary by re-mixing the soil in a food mixer with the required volume of Milli-Q water before returning the soil to the microcosm bottle and incubator.

3.4 Iodine extraction and analysis

After incubation for 114, 306, 810 and 3975 hours, samples (~4.5 g) of moist soil were equilibrated with 20 mL of 0.01 M KNO_3, followed by extraction with 0.15 M KH_2PO_4 and then 10 % TMAH, in 40 mL polycarbonate centrifuge tubes. At each stage soil suspensions were shaken for 16 hours on a reciprocal shaker, centrifuged (25 min at 3500 rpm), and filtered through 0.22 μm PTFE syringe filters. Calculation of phosphate-extractable iodine accounted for carry over from the previous KNO_3 equilibration gravimetrically. To follow shorter term iodine dynamics (< 72 hours), samples equivalent to ~3.5 g dry soil were taken from control microcosms and equilibrated in centrifuge tubes with 20 mL 0.01 M KNO_3 spiked with $^{129}I^-$ or $^{129}IO_3^-$ (0.15 mg kg^{-1} of soil) and shaken for a known time before centrifugation and filtration. Nitrate and phosphate extract solutions were analysed for dissolved organic carbon (DOC), iodine species ($^{127}I^-$, $^{127}IO_3^-$, $^{129}I^-$, and $^{129}IO_3^-$) and total ^{127}I and ^{129}I concentrations. TMAH extracts were analysed for total ^{127}I and ^{129}I only.

DOC was measured using a Shimadzu total organic carbon analyser (TOC-V_{CPH}) with a non-dispersive infrared detector in 'non-purgeable organic carbon' (NPOC) mode. Carbon standards (1000 μg mL^{-1} C) were prepared from oven-dried potassium hydrogen phthalate in MilliQ water. Iodine species $^{127}I^-$, $^{127}IO_3^-$, $^{129}I^-$, and $^{129}IO_3^-$ were assayed by ICP-MS following in-line chromatographic separation using a Dionex ICS-3000 ion chromatography system operated in isocratic mode with a Hamilton PRP-X100 anion exchange column (250 x 4.6 mm; 5 μm particle size). The mobile-phase (flow rate 1.3 mL min^{-1}) was 60 mmol L^{-1} NH_4NO_3, $1x10^{-5}$ mmol L^{-1} Na_2-EDTA, 2% methanol with pH adjusted to 9.5 with TMAH. Sample processing was undertaken using Plasmalab software with peaks of individual species manually integrated. A correction for ^{129}Xe on the ^{129}I signal was applied by measuring ^{131}Xe and refining the software correction factor, which is based solely on the isotope ratio ($^{129}Xe/^{131}Xe$), to allow for mass discrimination effects. Stock standards of $^{127}I^-$ and $^{127}IO_3^-$ (1000

mg L^{-1}) were prepared from oven-dried analytical grade potassium iodide or iodate in a matrix of 5% TMAH and stored at 4°C. Mixed $^{127}I^-$ and $^{127}IO_3^-$ working standards were prepared from stocks before analysis using the mobile-phase as diluent. Concentrations of $^{129}I^-$ and $^{129}IO_3^-$ were calculated from $^{127}I^-$ and $^{127}IO_3^-$ standard curves, according to Equation 1:

$$^{129}I_{conc} = {}^{129}I_{CPS} \times \frac{Kf}{{}^{127}I_{sens}} \quad (1)$$

where, $^{129}I_{conc}$ is $^{129}I^-$ or $^{129}IO_3^-$ concentration (µg L^{-1}), $^{129}I_{CPS}$ is the total counts per second of $^{129}I^-$ or $^{129}IO_3^-$, Kf is a measured mass correction factor (typically 1.085), $^{127}I_{sens}$ is $^{129}I^-$ or $^{129}IO_3^-$ sensitivity (counts per second for a concentration of 1 µg L^{-1}). A standard was repeatedly analyzed, after every six samples, to correct for instrumental drift. Any change in sensitivity between repeated standard analyses was applied linearly to the intervening samples. LOD was defined by the reproducibility of integration to be ~0.3 µg L^{-1} (~0.002 mg kg^{-1}).

3.5 ^{129}I recovery

Approximately 4000 hr after spiking with $^{129}I^-$ or $^{129}IO_3^-$ weighed samples of ~3 g (wet weight) of soil were extracted with 20 mL 10% TMAH at 70°C for 3 hours, centrifuged at 3500 rpm for 25 min and filtered. To ensure complete recovery of iodine, the extraction was repeated three times, followed by a further two washing steps using 20 mL of MilliQ water with shaking for 3 hours. Filtered supernatant solutions from each extraction step, including the two washing steps, were accumulated in 100 mL volumetric flasks and made to the mark with milliQ water. Total ^{127}I and ^{129}I concentrations were then determined using ICP-MS.

3.6 Modelling $^{129}I^-$ and $^{129}IO_3^-$ transformation kinetics

For each soil, the reduction in solution concentration (in 0.01 M KNO_3) of $^{129}IO_3^-$ and $^{129}I^-$ as a function of time was modeled using a range of kinetic expressions described briefly in Table 2. The 'first-order' models assume that reaction kinetics proceed either to an equilibrium position with respect to dissolved IO_3^- or I^- (reversible; RFO model) or to zero concentration of inorganic iodine (irreversible; IFO model). In addition, to allow for initially instantaneous adsorption, the models were tested with initial concentrations of $^{129}I^-$ or $^{129}IO_3^-$ (I_0) equal to (i) the total amount of ^{129}I added (i.e. 0.15 mg kg^{-1} soil) or (ii) a concentration determined by the application

of a partition coefficient (kd). The addition of the coefficient kd allows for instantaneous adsorption of inorganic iodine, possibly on metal oxide sites; the value of kd was optimized alongside the kinetic parameters.

The empirical Elovich equation has been shown to describe the reaction kinetics of a wide range of inorganic compounds with soils and soil components (Atkinson et al., 1970; Chien and Clayton, 1980; Martin and Sparks, 1983). It is characterised by a greater ability to describe kinetics over a wide range of timescales, in contrast to other models, because it includes both a constant term which effectively describes instantaneous adsorption and an exponential term. Echevarria et al., (1998) and Sinaj et al., (1999) applied an equation based on an infinite series of exponential terms to describe the progressive mixing of metal isotopes with the native soil metal pool - described here as the 'ISE' model.

Where diffusion or transport-controlled processes are the rate-limiting steps a parabolic diffusion expression (Par-diffn model) has been used previously (Chute and Quirk, 1967, Jardine and Sparks, 1984, Havlin et al., 1985). Application of the spherical diffusion equation (Sph-diffn model; e.g. Brown et al., 1971) assumes that reactions are controlled by diffusion into uniform spherical aggregates of adsorption surfaces (e.g. humic acid). It has been applied successfully to describe diffusion-controlled kinetics in minerals and soils (Cliff et al. 2002; Altfelder and Streck, 2006; Iznaga et al., 2007). Altfelder and Streck (2006) demonstrated the greater consistency of the spherical diffusion approach over a first order kinetic equation when parameterised for short time periods and applied to longer reaction times (days-months) because the rate constants of the first order approach are strongly time dependent unlike the diffusion approach. Thus predicting long-term behaviour on the basis of parameters derived at a shorter timescale using a first-order approach is particularly problematic (Altfeder & Streck, 2006).

All the models were optimised for individual soils by minimising the residual standard deviation (RSD) between modeled and experimental data, while systematically changing the values of model parameters, using the 'Solver' function in the software package Excel 2007. In addition, an attempt was made to fit a single spherical diffusion model to all soils simultaneously by relating model parameters to soil variables; this is described in section 4.6.

4. RESULTS AND DISCUSSION

4.1 Soil Characteristics

Measured soil characteristics are presented in Table 1. Soils from Sutton Bonington (SB) were typically lower in pH (4-7) and total iodine concentration (I_{tot} = 2-4 mg kg^{-1}) than those from Stoke Rochford (ST) (pH ~7, I_{tot} = 7.5-12 mg kg^{-1}). Woodland topsoils (SB-WT, ST-WT) and the Stoke Rochford grassland soil (ST-GT) had relatively large organic carbon contents (6-10%), and loss on ignition (LOI), than the arable soils. Carbonate content was greatest in soils from Stoke Rochford where the underlying geology is limestone. A value of 2.5% carbonate in the SB arable topsoil (SB-AT) may reflect liming shortly before sampling occurred. Iron and Mn oxide concentrations were typically higher in soils from the ST site.

4.2 Equilibration in 0.01 M KNO_3 solution

The progressive change in $^{129}IO_3^-$, $^{129}I^-$, and total ^{129}I concentrations in solution, following equilibration in 0.01 M KNO_3, are shown in Figures 1 & 2 for all nine soils; concentrations are expressed as mg kg^{-1} soil. The decline in total ^{129}I concentrations varied with soil type, incubation temperature and the nature of the spiked species ($^{129}I^-$ or $^{129}IO_3^-$). Typically, sorption of ^{129}I from solution was fastest in soils at higher temperatures with lower pH and higher organic carbon contents. Sorption was faster for $^{129}I^-$ than for $^{129}IO_3^-$ spiked soils; $^{129}I^-$ was generally undetectable in the solution phase within ~ 100 hrs of spike addition whereas $^{129}IO_3^-$ was still detectable in solution for most soils at >300 hr (at 10°C). Total ^{129}I concentrations in solution were always greater than those of the inorganic ^{129}I species, indicating rapid transformation of $^{129}I^-$ and $^{129}IO_3^-$ to unknown forms of soluble ^{129}I-org species. Concentrations of ^{129}I-org species (calculated by subtracting concentrations of inorganic species from total iodine) also decreased with time but persisted longer than the inorganic species resulting in an increasing proportion of ^{129}I-org species in the solution phase over time.

Figure 1 shows an apparent instantaneous loss of $^{129}IO_3^-$ from solution with measured concentrations below 0.15 mg kg^{-1} in all soils in < 1 hr. Greatest initial $^{129}IO_3^-$ adsorption was observed in the low pH, low organic carbon content soil (SB-WS, 69% at 10°C and 82% at 20°C) (Figure 1(i)). High iodate adsorption was also observed in soil ST-GT (47% and 52% at 10°C and 20°C, respectively) (Figure 1(d)) which had the highest measured iron-oxide content. For the remaining soils, the apparent adsorption at 1 hr was 20-36% of the spike

added. The slowest $^{129}IO_3^-$ loss was observed in the arable subsoil (SB-AS, Figure 1(f)) which has a low organic content and relatively high pH, with ~ 7% of the $^{129}IO_3^-$ spike detectable after 3975 hrs at 10°C. Of the $^{129}IO_3^-$ remaining in solution, 15-20% was converted to ^{129}I-org forms within 24 hrs. This proportion increased over time for most soils. The rate of conversion to ^{129}I-org was greatest in the low pH, high organic matter soil SB-WT where 60-80% of total ^{129}I remaining in solution after 48 hrs had been converted to organic iodine species. Within 800 hrs all of the $^{129}IO_3^-$ added to grassland and woodland soils had been converted to organic forms whereas in arable subsoils only 30% of the total ^{129}I was present in solution as organic complexes. Conversion of inorganic to organic iodine was also high where either pH was low or organic matter content high, seen by comparison of soils SB-GT (moderately organic and slightly acidic), ST-WT (highly organic and slightly alkaline), and ST-GT (highly organic and slightly acidic) (Figure 1(g),(a) & (d)). No evidence for $^{129}IO_3^-$ reduction in solution to $^{129}I^-$ was observed but this cannot be ruled out as concentrations of $^{129}I^-$ may be below detection limits (< 0.5 μg L^{-1}).

The rapid initial loss of $^{129}IO_3^-$, may be attributable to a combination of volatilization, electrostatic sorption on inorganic soil phases and rapid immobilization by reduction at sites on organic matter e.g. quinone groups. Volatilization of ^{129}I from solution is considered unlikely as such losses have been shown to be small in previous studies (e.g. Sheppard et al., 2004; Sheppard et al., 2006). Sorption of iodide and iodate to oxide phases is weak at pH>6 where sorption to organic matter dominates (see e.g. Sheppard and Thibault, 1992 and references therein) but has been reported up to pH 9.6 (Yoshida et al., 1992; Kaplan et al., 2000). Below pH 6 iodate sorption is predominantly to iron and aluminium oxides with iron oxides becoming increasingly important as pH drops (Whitehead, 1974b). Iodate is non-reactive toward organic matter and studies have shown that it is reduced to electrophilic species such HOI or I_2 before incorporation into the organic structure of humus (Francois, 1987a & b; Bichsel and von Gunten, 1999, 2000; Radlinger and Heumann, 2000; Warner et al., 2000; Reiller et al., 2006; Schlegel et al., 2006; Steinberg et al., 2008c). The reduction of iodate has been shown to be faster under acidic conditions (Brummer and Field, 1979); in soils, humic substances can reduce iodate due to their electron-donor characteristic (Wilson and Weber, 1979). In the current study the rate of loss of $^{129}IO_3^-$ from solution was higher in the low pH soils than in high pH ones where the organic carbon content was comparable (e.g. SB-WT/ST-GT and SB-WS/SB-AS) consistent with a mechanism involving iodate sorption onto oxide phases at low pH's as adsorption sites are not occupied by negatively charged soil organic

matter (Gallard et al., 2009). In soils with similar pH the rate of $^{129}IO_3^-$ loss from soil solution was higher in those with greater organic carbon contents, e.g. SB-WS compared to SB-WT and SB-AS compared to SB-GT, demonstrating the importance of organic carbon in reducing iodate to a species (e.g. HOI, I_2) whereby it can be converted into org-I species in solution or in the solid phases. The complete mechanism of each of these reactions (illustrated schematically in Figure 3) cannot be fully elucidated as no attempt was made to measure intermediate species in the reaction, however the rates of sorption and formation of soluble org-I are both rapid (< 1 hr).

Figure 2 shows the rate of conversion of $^{129}I^-$ to ^{129}I-org and the loss of ^{129}I from solution as a function of time. In the subsoils total iodine in solution remained close to spike levels at ~ 0.15 mg kg^{-1} after 1 hr but 20-30% of $^{129}I^-$ had been transformed to org-I. Highest rates of $^{129}I^-$ loss were observed in the woodland and grassland topsoils with high organic carbon contents (ST-WT, ST-GT and SB-WT) where no measurable concentration of $^{129}I^-$ was observed after 2, 3 and 8 hours respectively, at 10°C or 20°C. In general, solution phase $^{129}I^-$ concentration reduced most rapidly at higher temperatures and in the Stoke Rochford (ST) soils, with higher pH, carbonate, and Fe-oxide, compared to soils with comparable land-use from Sutton Bonington (SB). With soils sampled at the same location loss of $^{129}I^-$ from solution was fastest in soils with higher organic carbon contents. In samples spiked with $^{129}I^-$, no evidence for oxidation to $^{129}IO_3^-$ was observed but formation of ^{129}I-org species was rapid and the proportion of these species in solution increased over time. Conversion was most rapid in soils with higher pH and organic matter contents (ST-WT and ST-GT) where 100% was converted to ^{129}I-org within 3 and 8 hr respectively. In soils with a lower pH value conversion to org-I was most rapid in the woodland topsoil (SB-WT) taking 8 - 24 hr and slowest in the woodland and arable subsoils (SB-WS & SB-AS). In the woodland subsoil total conversion of $^{129}I^-$ to ^{129}I-org took >300 hr and in the arable subsoil ~ 12% of the total ^{129}I remained as $^{129}I^-$ after 810 hr. Both soils have approximately the same organic carbon and metal oxide content but pH values were ~3.9 for the woodland soil and 6.5 for the arable subsoil.

In order to interact with soil organic matter it has been shown that iodide must be oxidised to an intermediate such as I_2 or HOI (Warner et al., 2000; Reiller et al., 2006; Schlegel et al., 2006). Metal (Fe, Mn, Al) oxide phases and soil organic matter are both possible oxidising agents. Soil metal oxides have been shown to oxidise iodide in amounts proportional to their concentration, and inversely proportional to pH, in a reaction

that is thermodynamically favourable up to pH 7.5 (Allard et al., 2009; Fox et al., 2009; Gallard et al., 2009). Humic substances, which contain some electron acceptor sites, also act as oxidising agents for iodide (Blodau et al., 2009; Keller et al., 2009). Sheppard and Thibault (1992) described rapid loss of iodide from solution in organic soils as a first order reaction. However, they observed no evidence for specific bonding of iodide as the majority of iodide was found to be easily desorbable by water within a few days indicating weak retention in organic soils.

4.3 Phosphate Extraction

Phosphate has been effectively used as an extractant for specifically adsorbed anions such as sulphate (Delfosse et al., 2005), selenite (Stroud et al., 2010) and iodate (Whitehead, 1973b). In this study extraction with 0.16 M KH_2PO_4 was used to determine the amount of $^{129}IO_3^-$ and $^{129}I^-$ adsorbed on Fe/Mn oxides, implemented following KNO_3 equilibration at selected sampling times. Across all soils, iodine spikes and temperatures, the total amount of phosphate-extractable ^{129}I from spiked soils after ~100 hr was very low, between 0.0015 mg kg^{-1} (1%) and 0.014 mg kg^{-1} (~9%). The largest extractable concentrations were found in subsoils with low organic matter contents (SB-AS, ST-AS, and SB-WS), whereas the lowest levels of extractable ^{129}I were in the organic-rich topsoils (SB-WT, ST-WT, and ST-GT). Of the total ^{129}I extracted, the majority was inorganic iodine ($^{129}IO_3^-$ and $^{129}I^-$) for most soils. In the higher pH arable subsoil (ST-AS) ~90% was inorganic with slightly less in the lower pH arable subsoil (SB-AS). The woodland topsoil with a relatively high pH value (ST-WT) had the lowest amount of inorganic iodine (20-40%), perhaps due to greater solubility of humic acid at high pH. Over time the proportion of inorganic iodine in the extraction decreased for all soils as the ^{129}I became progressively assimilated into the organic pool.

In iodate-spiked soils, iodate ($^{129}IO_3^-$) was only detected in phosphate extracts of arable subsoils (SB-AS and ST-AS), where it represented less than 3% of the initial spike concentration. This provides strong evidence that the initial 'instantaneous' sorption seen for iodate-spiked soils may not be inorganic adsorption of IO_3^- ions on Fe/Mn oxides. Combining phosphate-extractable iodate concentrations with data from equilibration with 0.01M KNO_3 enables calculation of IO_3^- ion distribution coefficients (kd) for the arable subsoils. However, values of kd(IO_3^-) were significantly smaller than anticipated from the proportion of added iodate immediately sorbed from solution (Figures 1c and 1f). This may indicate that oxide phases are less important in rapid

adsorption of iodate than previously assumed. The overall trend seen in Figs 1 and 2 may arise simply from rapid organic fixation, until exhaustion of initially available reduction capacity subsequently produces a slower assimilation rate.

Whether ^{129}I was added as either $^{129}I^-$ or $^{129}IO_3^-$ measurable concentrations of phosphate-extractable iodide ($^{129}I^-$) were found (0.0025-0.01 mg kg^{-1}, 1.6 - 6.6 %) in all the soils. This suggests that iodide may be specifically adsorbed to some extent (i.e. adsorbed in the presence of 0.01 M NO_3^-) and is not a wholly conserved solute. It also indicates, for the $^{129}IO_3^-$-spiked soils, that iodide may be an intermediate in the overall process whereby iodate is assimilated into humus.

4.4 TMAH Extraction

Tetra methyl ammonium hydroxide (TMAH) has recently been shown to extract quantitatively the total iodine content from environmental samples e.g. soils, sediments, plants, and food (Watts & Mitchell, 2009). Alkaline extractants such as TMAH mobilise humic acids (and org-I) by negative charge generation and may also cause some degree of hydrolysis of org-I compounds. In addition TMAH releases iodate from specific sorption sites on Fe/Al hydrous oxides by replacement with hydroxide ions and negative charge generation on the oxide surface (Yamada et al., 1996). One advantage of TMAH over inorganic extractants such as NaOH or KOH is that high pH values can be achieved without increasing the salt concentration of the extraction solution and hence reducing the possibility of precipitation in the ICP torch and nebuliser during analysis.

A single TMAH (10%) extraction was used as a final step for some samples, following phosphate extraction. On average, total-^{129}I extracted ranged from 0.109 – 0.129 mg kg^{-1} (representing 73-86% recovery of the 0.15 mg kg^{-1} spike). Recovery was generally slightly worse in organic rich soils (e.g. 75-80% in ST-WT) and better in those with lower organic matter contents (e.g. arable subsoils, SB-AS and ST-AS, 85-90%). The amount of total ^{129}I extracted was unaffected by incubation temperature or the iodine species used for initial spiking. Consequently an exhaustive extraction procedure using three sequential extraction steps with 10% TMAH was undertaken on two soils (SB-WT and SB-AS) chosen to represent 'end members' in terms of soil properties (pH and %SOC). This more rigorous extraction produced c. 100% recovery of ^{129}I spikes and confirms that loss of ^{129}I from solution was due to sorption on soil components rather than volatilization.

4.5 Modelling $^{129}I^-$ and $^{129}IO_3^-$

Model parameters and residual standard deviations (RSD) for individual model fits are given in Tables 3 and 4 for iodate and iodide respectively. Comparisons of how well individual models fit for iodate and iodide across all soils is shown in Figure 4. For iodate, models in which no instantaneous adsorption was allowed (i.e. irreversible first order (IFO), infinite exponential (ISE), reversible first order (RFO) and parabolic diffusion) gave a poorer fit, with a greater range of RSD values, than those that incorporated a kd value (Figure 4a). The reversible first order + kd (RFO-kd), irreversible first order + kd (IFO-kd) and spherical diffusion + kd (Sph-Diffn-kd) models generated the best fits and the smallest range of RSD values across the soils. The Sph-Diffn-kd model gave marginally the lowest average RSD value overall (6.64 μg kg^{-1} c.f. 6.68 μg kg^{-1} for the IFO-kd model and 7.15 μg kg^{-1} for the RFO-kd model).

For iodide, with the exception of the ISE and Par-Diffn models, all models generated a similar average RSD value and the influence of instantaneous adsorption and requirement for inclusion of kd in the model was less clear. The reasons for this may be weaker adsorption of inorganic iodide on Fe/Mn oxides or a more *sustained* reaction with SOC in which either generation of intermediary iodine species is not limiting or diffusion into humic aggregates is faster. Also important to note is that the errors in the fits of iodide models are likely to be greater than those for iodate as the faster kinetics resulted in fewer measured values being obtained and fitted. The three iodide sorption models that generated the lowest RSD values are the same as those indentified as most successful in fitting iodate data i.e. reversible first order + kd (RFO-kd, average RSD 13.5 μg kg^{-1}), irreversible first order + kd (IFO-kd, average RSD 13.6 μg kg^{-1}) and spherical diffusion + kd (Sph-Diffn-kd, average RSD 14.2 μg kg^{-1}) (Figure 4b).

Reaction rate constants and distribution coefficients (kd values) calculated for all models are given in Tables 3 and 4 for iodate and iodide respectively. Comparison of the reaction rate constants generated by the irreversible first order model for soils incubated at 20°C with those incubated at 10°C showed that rates were on average 1.75 times higher at the higher temperature (Q_{10} = 1.75). The reaction rates for both iodate and iodide were greatest in the acidic woodland topsoil and subsoil (SB-WT and (SB-WS) and lowest in the organic-

poor, higher pH arable sub soil (SB-AS) from the same location, but there was no clear correlation with any individual soil property when reaction rates for individual soils were compared. Reaction rates for iodide were typically faster than those of iodate with the half life of iodide ranging from a minimum of 0.38 hr (ST-WT, 20^{o}C) to a maximum of 45 hr (SB-AS, 10^{o}C). Iodate half lives were longer, between 9 hr (SB-WT, 20^{o}C) and 412 hr (SB-AS, 10^{o}C). Modelled (optimized) kd values showed that instantaneous adsorption was usually greater for iodate than iodide.

IFO-kd and RFO-kd approaches described iodate and iodide reaction kinetics well, with the most important factor in achieving a good fit for iodate being the inclusion of a kd value to allow for instantaneous adsorption occurring at t=0. By contrast, for iodide, these models were only slightly better than those in which instantaneous adsorption was not included. An Elovich modeling approach, typically used to describe soil processes occurring across a range of timescales, generated a good fit for iodide but was less successful for iodate. Overall the best model fits to both iodate and iodide were achieved using a spherical diffusion approach. The success of the spherical diffusion model (Sph-Diffn-kd) for iodate appears to confirm its ability to describe processes over a relatively wide range of times (Altfelder and Streck 2006). That it also worked well for iodide suggests that it is useful for describing faster reaction kinetics as well. A comparison of modelled $^{129}I^{-}$ and $^{129}IO_3^{-}$ concentrations with experimentally measured concentrations for individual soils are shown in Figures 5 and 6 as a function of time.

4.6 Parameterising the spherical diffusion model from soil variables

An attempt was made to describe iodate sorption by all the soils based on a single spherical diffusion model parameterised from the soil variables: pH, soil organic carbon concentration (%SOC) and combined Fe+Mn oxide content (%Ox). Thus, the two parameters in Equation 8 (Table 2), kd and D/r^2, were expressed as functions of pH, %SOC and %Ox. The only apparent trends from fits of Equation 8 (Table 2) to individual soils were a linear relationship between $p(D/r^2)$ and %SOC and a weak exponential relation between kd and pH. For example, for incubations at 10^{o}C:

$$p\left(\frac{D}{r^2}\right) = 3.8 - 0.13(\%SOC); \quad r^2 = 0.67 \qquad (9)$$

and

$$kd = 17.0\exp(-0.28\,pH); \quad r^2 = 0.29 \tag{10}$$

The diffusion parameter, $p(D/r^2)$ was therefore expressed as a linear function of the three soil variables and the distribution coefficient (kd) as an exponential function of pH in which the value of kd at pH = 0 (ko) was a linear function of %SOC and %Ox:

$$p\left(\frac{D}{r^2}\right) = k_O + k_{pH}(pH) + k_C(\%SOC) + k_{ox}(\%Ox) \tag{11}$$

$$kd = [k_O + k_C(\%SOC) + k_{Ox}(\%Ox)]\exp(k_{pH}\,pH) \tag{12}$$

A single model fit was made (simultaneously) to all soils at each temperature (10°C and 20°C). Four combinations of the coefficients (k_O, k_{pH}, k_C and k_{Ox}) were tested, in the sequence listed, and overall values of RSD calculated (Table 5). In Table 5 the number of model parameters increases by four with each soil variable added because both $p(D/r^2)$ and kd were calculated as dependencies of the soil variables and the two temperature datasets are treated separately. Thus, with only k_O implemented all the soils at a given temperature are effectively ascribed average values for $p(D/r^2)$ and kd in which case the model fit was then optimised with four fitted coefficients. The two model parameters ($p(D/r^2)$ and kd) were also parameterised independently, producing model coefficient numbers between 4, 8, 12 and 16, but this produced broadly intermediate RSD values. Sequential addition of pH, %SOC and %Ox produced significant model improvements ($P<0.001$) in all cases. However, the inclusion of %SOC and %Ox in the calculation of kd value (Equation 12) does produce a potential instability in that it is possible to derive negative values for distribution coefficient at very large soil humus contents. Also, it was found that k_O applied to kd was reduced to zero when both %SOC and %Ox were included as variables to give 14, rather than 16, as the number of model coefficients required to give the best fit (Table 5). Table 6 shows the values of the soil coefficients used to derive the model parameters $p(D/r^2)$ and kd for each incubation temperature (Equations 11 and 12). For prediction of kd value, the soil coefficients are broadly in line with expectation in that kd declined with pH (k_{pH} is a negative exponential factor) and increases with Fe/Mn oxide content. This may reinforce the suggestion that the rapid

initial adsorption of iodate is as an inorganic species on hydrous oxides. Similarly, the negative values of k_c (for calculation of kd values) in Table 6 suggest that humus restricts the initial adsorption of iodate – possibly through competition for oxide sites and electrostatic repulsion. This agrees with the observation of Dai et al., (2004) who observed iodate adsorption to be positively correlated with free iron oxide content of soils and negatively correlated with soil organic matter content.

Figure 7 shows the fit of the soil-parameterised spherical diffusion model to iodate sorption. The overall simulation was reasonable across the range of soils examined with most soils falling wholly within ± 1 RSD of the 1:1 relation. However, some individual soils produced systematic deviation from the model trend. Thus, iodate persisted in solution in the SB-AS, a sandy arable subsoil with low soil organic carbon (%SOC) content, for longer than predicted by the model (at low iodate concentrations). The grassland topsoil from the same site showed the reverse trend with more rapid sorption from solution than predicted.

Apparent activation energies (Ea, kJ mol^{-1}) for each soil were determined from the intercept of a plot $\ln(D/r^2)$ against T^{-1}. The average value for eight of the soils was 42.7 ±3.4 kJ mol^{-1} with no significant relationship with %SOC (Figure 8), or soil pH value. The acidic woodland topsoil from Sutton Bonington (SB-WT), had extremely rapid reaction kinetics which showed very little temperature-dependence (Ea ≈ zero). Sparks (1989) presents approximate ranges for activation energies associated with different soil reaction-diffusion processes. Thus, a value for Ea just over 40 kJ mol^{-1} suggests a reaction process which is slower than simple pore diffusion (Ea ≈ 20 – 40 kJ mol^{-1}) or physical adsorption (8 – 25 kJ mol^{-1}) but at the lower end of surface reaction mechanisms. Figure 9a shows the effect of acidic conditions in soil (pH 4 vs pH 7) in causing pronounced instantaneous sorption of iodate, whether this is through rapid reduction of iodine to organic forms or adsorption of IO_3^- on Fe/Mn oxides. Increasing the (model) Fe/Mn oxide content also causes a greater initial fall in soluble iodate. Figure 9b shows (i) the influence of temperature in increasing the kinetic reaction but with minimal effect on the level of instantaneous sorption and (ii) in comparison with Fig. 9a, the increased rate of assimilation at greater soil humus content.

The main source of iodine to a soil is rainfall. The extent to which iodine in rainfall is retained by a soil will therefore depend not only on soil properties but also on factors including (i) distance from the ocean and

1 therefore iodine concentration in the rain, (ii) the speciation of iodine in the rainfall, (iii) the timing, duration
2 and intensity of the rainfall, (iv) whether the soil is dry or wet before a rainfall event, (v) the extent to which
3 the rainfall infiltrates or drains from a soil, which is dependent upon both the soil texture and its management
4 and soil temperature. Uptake by plant roots and microbial processing of the iodine may also be factors (see
5 e.g. Whitehead, 1975). Iodine concentration in rainfall is reported to be in the range of 0.5-5 μg L^{-1} (e.g.
6 Truesdale and Jones, 1996, Neal et al., 2007, Hou et al., 2009) but there is little agreement on the mix of
7 species present with I^-, IO_3^- and organic iodine all reported as 'major species', the relative proportions of each
8 varying with location (e.g. Gilfedder et al., 2007, Yoshida et al., 2007). Low intensity rainfall will infiltrate the
9 soil more easily than high intensity rainfall which 'seals' the surface of the soil increasing run-off. Coarse
10 textured (e.g. sandy) soils will allow easier infiltration (> 50 mm hr^{-1}) but will also drain completely within a few
11 hours whereas a fine textured (e.g. clayey) soil allows less infiltration (<15 mm hr^{-1}) and will take 2-3 days to
12 drain. For a shallow sandy soil with low organic matter content and a saturated hydraulic conductivity (K_{sat}) of
13 ~10 cm hr^{-1} it is possible that during a period of intense rainfall over several hours a substantial proportion of
14 rainfall iodine may be lost from the topsoil. Under typical rainfall conditions however, the rate of iodine
15 reactions in the topsoil are sufficiently rapid for the majority of the iodine to be retained in this layer. Figure
16 10 demonstrates retention of the iodine in the topsoil for the sandy loam soils from the Sutton Bonington sites
17 where measured iodine:carbon (I:C) ratios in soil are plotted as a function of depth for the woodland and
18 arable soil profiles. The I:C ratio increases with depth for both soils demonstrating that whilst the majority of
19 iodine is retained in the top soil the smaller amounts of humus present at depth have a high iodine
20 concentration compared to the more abundant organic matter in the topsoil. Thus iodine moving beyond the
21 topsoil during rainfall or drainage events appears to be effectively retained in the deeper soil horizons by the
22 substantial adsorption capacity provided by relatively small amounts of humus. The capacity of topsoil and
23 subsoil to effectively scavenge iodine from drainage water is supported by the low concentrations of iodine
24 (typically <5 μg L^{-1}) reported in river waters and the observation that iodine speciation in freshwater tends to
25 be dominated by organic forms (e.g. Reifenhauser & Heumann, 1990).
26
27
28

5. CONCLUSIONS

This study demonstrates that iodine added to soil is rapidly transformed from inorganic to organic forms. Transformation of inorganic iodine into organic forms occurs rapidly in the soil solution and the rate of loss of iodine from the soil solution is dependent upon its speciation, with iodide being lost more rapidly (minutes-hours) than iodate (hours-days) especially in high organic matter soils. The ultimate fate of iodine added to soil appears to be incorporation into soil organic matter via formation of intermediates e.g. HOI or I_2. Abiotic reduction of IO_3^-, or oxidation of I^- by solid or aqueous organic matter are likely to be the main mechanisms by which these intermediates are formed (although this work provides no specific evidence for this) as the reaction rates observed appear to be too fast for biological processes to play a significant role. It appears that inorganic adsorption of iodide and iodate plays only a minor, and probably transient, role in retention of iodine in soils. Rates of iodine loss are greater at higher temperatures with the rate almost doubling as temperatures increase from 10 to 20^{o}C.

Using a spherical diffusion modelling approach with instantaneous adsorption, that has been optimised across all the studied soils for iodate and iodide, this work demonstrates that it is possible to predict iodine behaviour as a function of pH, soil organic carbon, oxide content and temperature.

Acknowledgements

We acknowledge funding from the Natural Environment Research Council (Grant Ref: NE/H011684/1) to support this work. WHS also acknowledges a scholarship from the Egyptian Government. We thank the trustees of the Stoke Rochford Estate for permission to sample on the estate, and in particular Mr S. Allam the Estate Manager for his assistance in identifying suitable sampling sites. Org-C analysis was undertaken at the British Geological Survey and we are grateful to Vicky Moss-Hayes for her assistance with this.

6. REFERENCES

Abdel-Moati M.A.R. (1999) Iodine speciation in the Nile River estuary. *Marine Chem.,* **65,** 211-225.

Allard S., von Gunten U., Sahli E., Nicolau R. & Gallard H. (2009) Oxidation of iodide and iodine on birnessite (δ-MnO_2) in the pH range 4-8. *Water Res.,* **43,** 3417-3426.

Altfelder S. & Streck T. (2006) Capability and limitations of first-order and diffusion approaches to describe long-term sorption of chlortoluron in soil. *J. Contam. Hydrol.,* **86,** 279-298.

Atkinson R.J., Hingston F.J., Posner A.M. & Quirk J.P. (1970) Elovich equation for kinetics of isotopic exchange reactions at solid-liquid interfaces. *Nature,* **226,** 148-149.

Bichsel Y. & von Gunten U. (1999) Oxidation of iodide and hypoiodous acid in the disinfection of natural waters. *Env. Sci. Technol.,* **33,** 4040-4045.

Bichsel Y. & von Gunten U. (2000) Formation of iodo-trihalomethanes during disinfection and oxidation of iodide containing waters. *Env. Sci. Technol,* **34,** 2784-2791.

Blodau C., Bauer M., Regenspurg S. & Macalady D. (2009) Electron accepting capacity of dissolved organic matter as determined by reaction with metallic zinc. *Chem. Geol.,* **260,** 186-195.

Bonhoure I. Scheidegger A.M, Wieland E. & Dahn R. (2002) Iodine species uptake by cement and CSH studied by I K-edge X-ray absorption spectroscopy. *Radiochim. Acta*, **90**, 647-651.

Brown l.M., Sherry H.S. & Krambeck F.J. (1971) Mechanism and kinetics of isotopic exchange in zeolites. 1. Theory. *J. Phys. Chem.,* **75,** 3846-3855.

Brummer J. G. & FIeld R. J. (1979) Kinetics and mechanism of the oxidation of ferrous ion by iodate ion in strong perchloric-acid, aqueous-media. *J. Phys. Chem.,* **83,** 2328-2335.

Chien S. H. & Clayton W. R. (1980) Application of Elovich equation to the kinetics of phosphate release and sorption in soils. *Soil Sci. Soc. Am. J.,* **44,** 265-268.

Chute J.H. & Quirk J.P. (1967) Diffusion of potassium from mica-like clay minerals. *Nature,* **213,** 1156-&.

Cliff J.B., Bottomley P.J., Haggerty R. & Myrold D.D. (2002) Modeling the effects of diffusion limitations on nitrogen-15 isotope dilution experiments with soil aggregates. Soil *Sci. Soc. Am. J.,* **66,** 1868-1877.

Dai J. L., Zhang M., Hu Q.H., Huang Y.Z., Wang R.Q. & Zhu Y.G. (2009) Adsorption and desorption of iodine by various chinese soils: II. Iodide and iodate. *Geoderma,* **153,** 130-135.

Dai J. L., Zhang M. & Zhu Y. G. (2004) Adsorption and desorption of iodine by various chinese soils - I. Iodate. *Environ. Int.,* **30,** 525-530.

Delfosse T., Delmelle P., Givron C. & Delvaux B. (2005) Inorganic sulphate extraction from SO_2-impacted andosols. *Eur. J. Soil Sci.,* **56,** 127-133.

Echevarria G., Morel J.L., Fardeau J.C. & Leclerc-Cessac E. (1998) Assessment of phytoavailability of nickel in soils. *J. Env. Qual.,* **27,** 1064-1070.

Fox P.M., Davis J.A. & Luther G.W. (2009) The kinetics of iodide oxidation by the manganese oxide mineral birnessite. *Geochim. Cosmochim. Acta,* **73,** 2850-2861.

Francois R. (1987a) The influence of humic substances on the geochemistry of iodine in nearshore and hemipelagic marine-sediments. *Geochim. Cosmochim. Acta,* **51,** 2417-2427.

Francois, R. (1987b) Iodine in marine sedimentary humic substances. *Sci. Tot. Envion.,* **62,** 341-342.

Fukui M., Fujikawa Y. & Satta N. (1996) Factors affecting interaction of radioiodide and iodate species with soil. *J. Env. Rad.,* **31,** 199-216.

Furhmann M., Bajt S., & Schoonen M.A.A. (1998) Sorption of iodine on minerals investigated by X-ray absorption near edge structure (XANES) and ^{125} I tracer sorption experiments. *Appl. Geochem*., **13**, 127-141

Gallard H., Allard S., Nicolau R., von Gunten U. & Croue J. P. (2009) Formation of iodinated organic compounds by oxidation of iodide-containing waters with manganese dioxide. *Env. Sci. Technol.,* **43,** 7003-7009.

Geelhoed J.S., Hiemstra T. & VanreimsdiJk W.H. (1997) Phosphate and sulfate adsorption on goethite: Single anion and competitive adsorption. *Geochim. Cosmochim. Acta,* **61,** 2389-2396.

Gilfedder B.S., Petri M. & Biester H. (2007a) Iodine and bromine speciation in snow and the effect of orographically induced precipitation. *Atmos. Chem. Phys.,* **7,** 2661-2669.

Gilfedder B S., Petri M. & Biester H. (2007b) Iodine speciation in rain and snow: Implications for the atmospheric iodine sink. *J. Geophys. Res. - Atmos.,* 112, 1-7.

Gilfedder B.S. Lai S.C., Petri M., Biester H. & Hoffmann T. (2008) Iodine speciation in rain, snow and aerosols. *Atmos. Chem. Phys*. **8**, 6069-6084.

Havlin J.L., Westfall D.G. & Olsen S.R. (1985) Mathematical-models for potassium release kinetics in calcareous soils. *Soil Sci. Soc. Am. J.,* **49,** 371-376.

Hou X.L., Aldahan A., Nielsen S.P. & Possnert G. (2009) Time Series of I-129 and I-127 Speciation in Precipitation from Denmark. *Environmental Science & Technology,* **43,** 6522-6528.

Iznaga I. R., Petranovskii V., Fuentes G.R., Mendoza C. & Aguilar, A.B. (2007) Exchange and reduction of Cu^{2+} ions in clinoptilolite. *J. Colloid Interf. Sci.,* **316,** 877-886.

Jardine P.M. & Sparks D.L. (1984) Potassium-calcium exchange in a multireactive soil system. 1. Kinetics. *Soil Sci. Soc. Am. J.,* **48,** 39-45.

Johnson C.C. (2003) The geochemistry of iodine and its application to environmental strategies for reducing the risks from iodine deficiency disorders (idd). *British Geological Survey,* DFID kar project R7411**,** Report CR/03/057N.

Johnson C.C., Breward N., Ander E.L. & Ault L. (2005) G-BASE: Baseline geochemical mapping of Great Britain and Northern Ireland. *Geochemistry: Exploration, Environment, Analysis* **5**, 347-357.

Johnson C.C., Strutt M.H, Hmeurras M. & Mounir M. (2002) Iodine in the environment of the high atlas mountain area of Morocco. *British Geological Survey,* DFID kar project R7411**,** Report CR/02/196N.

Kaplan D. I., Serne R. J., Parker K. E. & Kutnyakov I. V. (2000) Iodide sorption to subsurface sediments and illitic minerals. *Env. Sci. Technol.,* **34,** 399-405.

Keller J. K., Weisenhorn P. B. & Megonigal J. P. (2009) Humic acids as electron acceptors in wetland decomposition. *Soil Biol. Biochem.,* **41,** 1518-1522.

Kodama S., Takahashi Y., Okumura K. & Uruga T. (2006) Speciation of iodine in solid environmental samples by iodine K-edge XANES: Application to soils and ferromanganese oxides. *Sci. Tot. Environ.,* **363**, 275-284.

Kostka J.E. & Luther G.W. (1994) Partitioning and speciation of solid-phase iron in salt-marsh sediments. *Geochimica Cosmochim. Acta,* **58,** 1701-1710.

Liu W., Yang H.X., Li B., Chen D.Y. & Zhang H.J. (2007) Study on speciation stabilities of iodine in underground water by high performance liquid chromatography-inductively coupled plasma mass spectrometry. *Chinese J. Anal. Chem.,* **35,** 571-574.

Low M.J.D. (1960) Kinetics of chemisorption of gases on solids. *Chem. Rev.,* **60,** 267-312.

Martin H.W. & Sparks D.L. (1983) Kinetics of non-exchangeable potassium release from two coastal-plain soils. *Soil Sci. Soc. Am. J.,* **47,** 883-887.

Muramatsu Y., Yoshida S., Fehn U., Amachi S. & Ohmomo Y. (2004) Studies with natural and anthropogenic iodine isotopes: iodine distribution and cycling in the global environment. *J. Env. Rad.,* **74,** 221-232.

Neal C., Neal M., Wickham H., Hill L. & Harman S. (2007) Dissolved iodine in rainfall, cloud, stream and groundwater in the Plynhmon area of mid-Wales. *Hydrol. Earth System Sci.,* **11,** 283-293.

Piper C.S. (1954) Soil and Plant Analysis : A laboratory manual of methods for the examination of soils and the determination of the inorganic constituents of plants. *International Science Publisher Inc., New York*.

Radlinger G. & Heumann K.G. (1997) Determination of halogen species of humic substances using HPLC/ICP-MS coupling. *Fresenius J. Anal. Chem.,* **359,** 430-433.

Radlinger G. & Heumann K. G. (2000) Transformation of iodide in natural and wastewater systems by fixation on humic substances. *Env. Sci. Technol.,* **34,** 3932-3936.

Reifenhauser C. & Heumann K.G. (1990) Development of a definitive method for iodine speciation in aquatic systems. *Fresnius J. Anal. Chem.* **336**, 559-563.

Reiller P., Mercier-Bion F., Gimenez N., Barre N. & Miserque F. (2006) Iodination of humic acid samples from different origins. *Radiochim. Acta,* **94,** 739-745.

Schlegel M.L., Reiller P., Mercier-Bion F., Barre N. & Moulin V. (2006) Molecular environment of iodine in naturally iodinated humic substances: Insight from X-ray absorption spectroscopy. *Geochim. Cosmochim. Acta,* **70,** 5536-5551.

Schwehr K.A. & Santschi P.H. (2003) Sensitive determination of iodine species, including organo-iodine, for freshwater and seawater samples using high performance liquid chromatography and spectrophotometric detection. *Anal. Chim. Acta,* **482,** 59-71.

Sheppard M.I., Hawkins J.L. & Smith P.A. (1996) Linearity of iodine sorption and sorption capacities for seven soils. *J. Env. Qual.,* **25,** 1261-1267.

Sheppard M. I. & Thibault D. H. (1992) Chemical behavior of iodine in organic and mineral soils. *Appl. Geochem.,* **7,** 265-272.

Sheppard M.I., Thibault D.H., Smith P.A.& Hawkins J.L. (2004) Volatilization: A Soil Degassing Coefficient for Iodine. *J. Environ. Radioactivity* **25**, 189-203.

Sheppard S.C., Sheppard M.I., Tait J.C. & Sanipelli B.L. (2006) Revision and meta-analysis of selected biosphere parameter values for chlorine, iodine, neptunium, radium, radon and uranium. *J. Environ. Radioactivity* **89**, 115-137

Sinaj S., Machler F. & Frossard E. (1999) Assessment of isotopically exchangeable zinc in polluted and nonpolluted soils. *Soil Sci. Soc. Am. J.,* **63,** 1618-1625.

Smith J.D. & Butler E.C.V. (1979) Speciation of dissolved iodine in estuarine waters. *Nature,* **277,** 468-469.

Sparkes D.L. (1989) Kinetics of Soil Chemical Processes. *Academic Press, inc.,* San Diego, California 92101, USA.

1 Sparkes D.L. (2003) Environmental Soil Chemistry. *Academic Press, inc.,* San Diego, California, 92101-4495, USA.
2 Steinberg S.M., Buck B., Morton J. & Dorman J. (2008a) The speciation of iodine in the salt impacted black
3 butte soil series along the virgin river, Nevada, USA. *Appl. Geochem.,* **23,** 3589-3596.
4 Steinberg S.M., Kimble G.M., Schmett G.T., Emerson D.W., Turner M.F. & Rudin M. (2008b) Abiotic reaction of
5 iodate with sphagnum peat and other natural organic matter. *J. Radioanal. Nucl. Chem.,* **277,** 185-191.
6 Steinberg S.M., Schmett G.T., Kimble G., Emerson D.W., Turner M.F. & Rudin M. (2008c) Immobilization of
7 fission iodine by reaction with insoluble natural organic matter. *J. Radioanal. Nucl. Chem.,* **277,** 175-183.
8 Stroud, J.L., Broadley, M.R., Foot, I., Fairweather-Tait, S.J., Hart, D.J., Hurst, R., Knott, P., Mowat, H., Norman, K.,
9 Scott, P., Tucker, M., White, P.J., McGrath, S.P. and Zhao, F.J. (2010) Soil factors affecting selenium
10 concentration in wheat grain and the fate and speciation of Se fertilisers applied to soil. Plant and Soil, **332**,
11 19-30.
12 Trotter W.R. (1960) The association of deafness with thyroid dysfunction. *British Medical Bulletin,* **16,** 92-98.
13 Truesdale V.W. & Jones S.D. (1996) The variation of iodate and total iodine in some UK rainwaters during 1980-
14 1981. *J. Hydrol.,* **179,** 67-86.
15 Underwood E.J. (1977) Iodine. *Trace Elements in Human and Animals.* 4th ed. Nueva York, Academic Press,
16 p:271-301.
17 Warner J.A., Casey W.H. & Dahlgren R.A. (2000) Interaction kinetics of $I_{2(aq)}$ with substituted phenols and humic
18 substances. *Env. Sci. Technol.,* **34,** 3180-3185.
19 Watts M.J. & Mitchell C.J. (2009) A pilot study on iodine in soils of Greater Kabul and Nangarhar provinces of
20 Afghanistan. *Env. Geochem. Health,* **31,** 503-509.
21 Whitehead D.C. (1973a) Sorption of iodide by soils as influenced by equilibrium conditions and soil properties.
22 *J. Sci.Fd Agric.,* **24,** 547-556.
23 Whitehead D. C. (1973b) Studies on iodine in British soils. *J. Soil Sci.,* **24,** 260-270.
24 Whitehead D.C. (1974a) Sorption of iodide by soil components. *J. Sci.Fd Agric.,* **25,** 73-79.
25 Whitehead D.C. (1974b) Influence of organic-matter, chalk, and sesquioxides on solubility of iodide, elemental
26 iodine, and iodate incubated with soil. *J. Soil Sci.,* **25,** 461-470.
27 Whitehead D.C. (1975) Uptake by perennial ryegrass of iodide, elemental iodine and iodate added to soil as
28 influenced by various amendments, *J. Sci. Fd. Agric.*, **26**, 361-367.

Whitehead D.C. (1978) Iodine in soil profiles in relation to iron and aluminum-oxides and organic-matter. *J. Soil Sci.,* **29,** 88-94.

WHO (2004) *In*; Benoist B. et al. (Eds).Iodine status worldwide. *Department of Nutrition for Health and Development, World Health Organization.* Geneva.

Wilson S.A. & Weber, J.H. (1979) EPR study of the reduction of vanadium(V) to vanadium(IV) by fulvic-acid. *Chem. Geol.,* **26,** 345-354.

Yamada H., Kiriyama T. & Yonebayashi K. (1996) Determination of total iodine in soils by inductively coupled plasma mass spectrometry. *Soil Sci. Plant Nut.,* **42,** 859-866.

Yamaguchi N., Nakano M., Takamatsu R. & Tanida H. (2010) Inorganic iodine incorporation into soil organic matter: Evidence from iodine k-edge X-ray absorption near-edge structure. *J. Env. Radioactivity,* **101,** 451-457.

Yang H.X., Liu W., Li B., Zhang H.J., Liu X.D. & Chen D.Y. (2007) Speciation analysis for iodine in groundwater using high performance liquid chromatography-inductively coupled plasma-mass spectrometry (HPLC-ICP-MS). *Geostand. Geoanal. Res.,* **31,** 345-351.

Yntema l.F. & Fleming T. (1939) Volumetric oxidation of iodide to iodate by sodium chlorite. *Industrial and Engineering Chemistry-Analytical Edition,* **11,** 375-377.

Yoshida S., Muramatsu Y., Katou S. & Sekimoto H. (2007) Determination of the chemical forms of iodine with IC-ICP-MS and its application to environmental samples. *J. Radioanal. Nucl. Chem.,* **273,** 211-214.

Yoshida S., Muramatsu Y. & Uchida S. (1992) Studies on the sorption of I^-(iodide) and IO_3^-(iodate) onto andosols. *Water Air Soil Pollution,* **63,** 321-329.

Yu Z.S., Warner J.A., Dahlgren R.A. & Casey W.H. (1996) Reactivity of iodide in volcanic soils and noncrystalline soil constituents. *Geochim. Cosmochim. Acta,* **60,** 4945-4956.

Table 1: Summary of soil properties. Standard error for triplicate measurements is shown in brackets after the number.

Soil	Code	pH	^{127}I Mean (mg/kg)	Org-C Mean %	LOI Mean %	Carbonate Mean %	$Al(OH)_3$ Mean %	MnO_2 Mean %	Fe_2O_3 Mean %	Moisture content of incubated soil % dry wt
Stoke Rochford Woodland Topsoil	**ST-WT**	7.2	9.07 (*0.04*)	5.93	16.8 (*0.12*)	42.8 (*0.99*)	0.226 (*0.002*)	0.063 (*0.0004*)	1.76 (*0.02*)	37.6
Stoke Rochford Arable Topsoil	**ST-AT**	7.34	7.48 (*0.09*)	2.88	9.04 (*0.22*)	5.37 (*0.34*)	0.361 (*0.004*)	0.061 (*0.0005*)	2.08 (*0.01*)	19.2
Stoke Rochford Arable Subsoil	**ST-AS**	7.05	9.72 (*0.06*)	2.41	9.37 (*0.19*)	6.65 (*0.46*)	0.481 (*0.007*)	0.084 (*0.0004*)	2.80 (*0.08*)	16.8
Stoke Rochford Grassland Topsoil	**ST-GT**	6.85	11.8 (*0.10*)	8.39	20.1 (*0.15*)	1.47 (*0.36*)	0.505 (*0.018*)	0.094 (*0.0005*)	3.56 (*0.21*)	40.3
Sutton Bonington Arable Topsoil	**SB-AT**	6.98	4.87 (*0.10*)	2.24	6.56 (*0.18*)	2.50 (*0.12*)	0.283 (*0.001*)	0.040 (*0.0002*)	1.49 (*0.01*)	18.5
Sutton Bonington Arable Subsoil	**SB-AS**	6.50	2.35 (*0.02*)	0.79	3.54 (*0.07*)	0.00 (*0.00*)	0.241 (*0.003*)	0.026 (*0.0004*)	1.28 (*0.02*)	11.7
Sutton Bonington Grassland Topsoil	**SB-GT**	6.63	2.57 (*0.07*)	2.44	5.89 (*0.10*)	0.00 (*0.00*)	0.195 (*0.001*)	0.022 (*0.0002*)	1.00 (*0.01*)	17.7
Sutton Bonington Woodland Topsoil	**SB-WT**	4.38	4.41 (*0.12*)	10.14	23.4 (*0.39*)	0.00 (*0.00*)	0.286 (*0.003*)	0.011 (*0.0002*)	1.07 (*0.004*)	57.0
Sutton Bonington Woodland Subsoil	**SB-WS**	3.86	1.98 (*0.06*)	1.66	4.4 (*0.73*)	0.00 (*0.00*)	0.243 (*0.001*)	0.007 (*0.0001*)	1.02 (*0.01*)	13.5

Table 2: Equations used to model the transformation kinetics of $^{129}I^-$ or $^{129}IO_3^-$

Model	Equation			Reference
Irreversible First Order (IFO)	$I_t = I_0\, e^{-kt}$	(2)	I_t is the concentration of $^{129}I^-$ or $^{129}IO_3^-$ in solution at time t (mg kg^{-1} soil), k is the reaction rate constant (hr^{-1}), t is time (h) and I_0 is the total concentration of $^{129}I^-$ or $^{129}IO_3^-$ at time t =0. I_{tot} is the total concentration of $^{129}I^-$ or $^{129}IO_3^-$ (amount added,mg kg^{-1} soil), W is the soil mass (g), V is the solution volume (mL) and $k_{d(0)}$ is apparent distribution coefficient of $^{129}I^-$ or $^{129}IO_3^-$ at time t = 0	see e.g. Sparkes (1989)
	and $I_0 = \frac{I_{tot}}{1 + K_{d(0)}\frac{W}{V}}$	(3)		
Reversible First Order (RFO)	$I_t = I_{t-1}(1-k_F) + k_R(I_0 - I_{t-1})$	(4)	I_{t-1} is the concentration of $^{129}I^-$ or $^{129}IO_3^-$ (mg kg^{-1} soil) in solution at time t_{-1}, and k_F and k_R are the forward and reversible reaction rate constants (hr^{-1}), respectively.	Empirical
Elovich	$I_t = I_0 - \left(\frac{1}{\beta}\ln \alpha\beta + \frac{1}{\beta}\ln t\right)$	(5)	α and β are constants	see e.g. Chien and Clayton (1980)
Infinite series exponential (ISE)	$I_t = I_0\left(t + I_0^{1/\alpha}\right)^{-\alpha}$	(6)	α is a constant	see e.g. Sinaj et al. (1999)
Parabolic Diffusion (Par-Diffn)	$I_t = I_0(1 - R_D\sqrt{t} + \alpha)$	(7)	R_D is the overall diffusion coefficient and α is a constant	see e.g. Sparkes (2003)
Spherical Diffusion (Sph-Diffn)	$I_t = I_0\left(\frac{6}{\pi^2}\sum_{n=1}^{n=\infty}\frac{1}{n^2}\exp -\left(\frac{n^2\pi^2 Dt}{r^2}\right)\right)$	(8)	n is an integer, D is the intra-aggregate diffusion coefficient ($m^2\ hr^{-1}$) and r is the aggregate radius (m)	see e.g. Brown et al. (1971)

Table 3: Summary of iodate model outputs for each soil type at 10°C and 20°C. For a definition of each parameter please see Table 2. Quoted residual standard deviations are the average for both temperatures.

	ST-WT		ST-GT		ST-AT		ST-AS		SB-WT		SB-WS		SB-AT		SB-AS		SB-GT	
	10°C	20°C	10°C	20°C	10°C	20°C	10°C	20°C	10°C	20°C	10°C	20°C	10°C	20°C	10°C	20°C	10°C	20°C
Parabolic Diffusion																		
RD - overall diffn coeff	0.021	0.021	0.017	0.018	0.010	0.010	0.009	0.009	0.016	0.016	0.004	0.004	0.012	0.012	0.008	0.010	0.027	0.028
Constant	0.529	0.577	0.603	0.624	0.488	0.527	0.530	0.536	0.694	0.705	0.821	0.815	0.396	0.448	0.466	0.446	0.361	0.383
RSD ($\mu g\ kg^{-1}$)	*23.37*		*17.14*		*25.08*		*17.40*		*24.49*		*13.22*		*29.11*		*15.30*		*21.98*	
Elovich																		
α	0.574	0.610	5.785	2.835	0.284	0.370	2.093	0.719	4.560	6.191	948404	48898	0.085	0.078	1.189	0.223	0.115	0.097
β	65.812	62.437	85.088	75.376	74.089	72.727	94.896	80.816	74.085	76.126	175.144	151.576	67.495	60.177	100.097	76.886	59.066	53.846
RSD ($\mu g\ kg^{-1}$)	*9.40*		*6.84*		*15.44*		*8.61*		*12.30*		*5.89*		*19.36*		*9.24*		*17.56*	
Irreversible 1st order + Kd																		
kd (L kg^{-1})	3.514	3.163	5.776	4.863	3.008	2.735	5.015	3.635	4.094	4.368	13.759	11.615	2.122	1.579	4.259	2.910	2.180	1.857
Rate const (hr^{-1})	0.017	0.028	0.014	0.023	0.006	0.009	0.003	0.007	0.069	0.069	0.013	0.017	0.005	0.009	0.002	0.004	0.010	0.014
RSD ($\mu g\ kg^{-1}$)	*6.24*		*6.12*		*6.46*		*9.10*		*3.40*		*4.90*		*6.84*		*8.98*		*8.09*	
Irreversible 1st order																		
Rate const (hr^{-1})	0.041	0.275	0.413	0.381	0.015	0.018	0.018	0.020	0.282	0.302	0.959	0.851	0.010	0.014	0.013	0.013	0.017	0.021
RSD ($\mu g\ kg^{-1}$)	*26.68*		*25.39*		*28.64*		*35.35*		*16.78*		*16.96*		*23.00*		*33.23*		*24.36*	
Reversible 1st order + kd																		
kd (L kg^{-1})	3.487	3.161	5.682	4.843	2.965	2.735	4.811	3.466	4.035	4.350	7.194	11.580	2.122	1.579	3.526	2.748	2.180	1.857
Forward Rate constant (hr-1)	0.018	0.028	0.014	0.023	0.006	0.009	0.003	0.008	0.069	0.067	0.224	0.017	0.004	0.009	0.004	0.005	0.010	0.014
Reverse Rate constant (hr-1)	0.000	0.000	0.001	0.000	0.000	0.000	0.000	0.001	0.001	0.000	0.054	0.000	0.000	0.000	0.001	0.001	0.000	0.000
RSD ($\mu g\ kg^{-1}$))	*6.78*		*6.53*		*6.85*		*9.04*		*3.61*		*8.17*		*7.39*		*7.16*		*8.86*	
Reversible 1st order																		
Forward Rate constant (hr^{-1})	0.263	0.254	0.389	0.341	0.229	0.231	0.310	0.253	0.271	0.287	0.660	0.621	0.189	0.014	0.274	0.015	0.201	0.021
Reverse Rate constant (hr^{-1})	0.049	0.028	0.072	0.042	0.085	0.071	0.117	0.081	0.014	0.015	0.065	0.057	0.096	0.000	0.147	0.002	0.075	0.000
RSD ($\mu g\ kg^{-1}$)	*20.12*		*18.81*		*33.28*		*24.92*		*16.62*		*12.36*		*31.26*		*26.20*		*30.10*	
Inf-exp + kd																		
kd (L kg^{-1})	2.395	2.228	4.285	3.627	1.725	2.039	2.799	2.191	3.440	3.705	10.745	9.254	1.086	0.809	2.249	1.557	1.424	1.176
Constant (n)	0.312	0.399	0.277	0.358	0.204	0.219	0.174	0.212	0.486	0.490	0.282	0.317	0.181	0.234	0.141	0.178	0.228	0.271
RSD ($\mu g\ kg^{-1}$)	*12.30*		*10.32*		*21.56*		*13.97*		*9.90*		*6.16*		*26.26*		*15.05*		*24.50*	
Inf-exp																		
Constant (n)	0.441	0.565	0.511	1.335	0.271	0.297	0.279	0.300	1.102	1.251	2.609	2.466	0.222	0.267	0.223	0.237	0.289	0.325
RSD ($\mu g\ kg^{-1}$)	*22.47*		*28.09*		*26.84*		*25.05*		*21.37*		*17.30*		*26.75*		*24.72*		*26.59*	
Spherical Diffusion + kd																		
kd (L kg^{-1})	2.328	1.814	4.420	3.358	2.116	1.925	3.816	2.698	2.218	1.156	11.449	9.325	1.337	0.819	3.285	2.086	1.360	0.987
D/r^2	0.001	0.002	0.001	0.002	0.000	0.001	0.000	0.000	0.005	0.005	0.001	0.001	0.000	0.001	0.000	0.000	0.001	0.001
RSD ($\mu g\ kg^{-1}$)	*5.11*		*4.72*		*8.88*		*6.75*		*2.67*		*4.44*		*10.72*		*5.69*		*10.80*	

Table 4: Summary of iodide model outputs for each soil type at 10°C and 20°C. For a definition of each parameter please see Table 2. Quoted residual standard deviations are the average for both temperatures.

	ST-WT		ST-GT		ST-AT		ST-AS		SB-WT		SB-WS		SB-AT		SB-AS		SB-GT	
	10°C	20°C	10°C	20°C	10°C	20°C	10°C	20°C	10°C	20°C	10°C	20°C	10°C	20°C	10°C	20°C	10°C	20°C
Parabolic Diffusion																		
RD - overall diffn coeff	0.6606	0.4923	0.4740	0.4592	0.1580	0.3944	0.1201	0.1773	0.2594	0.1462	0.0294	0.0832	0.1092	0.1410	0.0295	0.0273	0.1145	0.1261
Constant	0.0386	0.3329	0.0728	0.2121	0.2554	0.1176	0.2376	0.1355	0.2070	0.3137	0.3901	0.1315	0.2914	0.4062	0.3570	0.4446	0.2067	0.2796
RSD ($\mu g\ kg^{-1}$)	*4.84*		*14.01*		*23.80*		*24.17*		*13.68*		*24.13*		*23.50*		*30.12*		*20.27*	
Elovich																		
α	0.437	1.075	0.338	0.564	0.148	0.366	0.146	0.090	0.308	0.332	0.065	0.048	0.188	0.530	0.066	0.100	0.096	0.174
β	20.01	26.51	25.01	25.77	31.02	30.16	40.76	27.86	32.78	39.07	46.89	40.50	42.31	38.89	50.11	49.05	36.22	38.10
RSD ($\mu g\ kg^{-1}$)	*4.68*		*14.90*		*20.09*		*16.39*		*11.23*		*15.53*		*17.12*		*18.84*		*13.33*	
Irreversible 1st order + Kd																		
kd (L kg^{-1})	0.214	0.958	1.133	1.693	0.460	1.532	1.892	0.000	1.801	1.995	1.416	1.357	1.193	1.867	1.631	1.690	1.685	1.113
Rate const (hr^{-1})	1.2721	1.8129	0.5999	0.8722	0.2509	0.4448	0.0804	0.2139	0.2940	0.2085	0.0219	0.0228	0.1455	0.3512	0.0156	0.0259	0.0660	0.1680
RSD ($\mu g\ kg^{-1}$)	*6.27*		*14.09*		*17.57*		*16.83*		*9.95*		*9.47*		*18.05*		*11.50*		*18.28*	
Irreversible 1st order																		
Rate const (hr^{-1})	1.3213	2.0751	0.7682	1.1638	0.2872	0.6474	0.1839	0.2139	0.5013	0.4168	0.0323	0.0331	0.2281	0.5764	0.0236	0.0408	0.1467	0.2458
RSD ($\mu g\ kg^{-1}$)	*5.39*		*14.24*		*16.95*		*17.10*		*15.94*		*19.65*		*18.89*		*22.15*		*19.51*	
Reversible 1st order + kd																		
kd (L kg^{-1})	0.214	0.958	1.217	1.780	0.346	1.473	0.516	0.000	1.698	1.892	1.417	1.357	0.196	1.977	1.631	1.690	0.723	0.274
Forward Rate constant (hr^{-1})	0.9412	1.1921	0.5055	0.6948	0.2497	0.4168	0.1813	0.2056	0.2878	0.2102	0.0217	0.0226	0.2516	0.3093	0.0154	0.0256	0.1234	0.2392
Reverse Rate constant (hr^{-1})	0.0000	0.0000	0.0000	0.0000	0.0153	0.0429	0.0603	0.0175	0.0197	0.0154	0.0000	0.0000	0.0772	0.0000	0.0000	0.0000	0.0211	0.0533
RSD ($\mu g\ kg^{-1}$)	*8.87*		*17.23*		*22.40*		*8.91*		*11.01*		*10.37*		*13.76*		*12.42*		*16.17*	
Reversible 1st order																		
Forward Rate constant (hr^{-1})	0.9670	1.2914	0.6891	0.9017	0.2770	0.6557	0.2197	0.2056	0.4872	0.4089	0.0332	0.0382	0.2690	0.5121	0.0240	0.0416	0.1697	0.2615
Reverse Rate constant (hr^{-1})	0.0000	0.0000	0.0810	0.0265	0.0185	0.1709	0.0679	0.0175	0.0745	0.0533	0.0008	0.0035	0.0795	0.0245	0.0005	0.0009	0.0300	0.0567
RSD ($\mu g\ kg^{-1}$)	*6.60*		*16.16*		*18.43*		*7.25*		*15.71*		*20.95*		*15.56*		*23.61*		*13.47*	
Inf-exp + kd																		
kd (L kg^{-1})	14.54	29.91	7.47	13.27	1.63	6.16	1.72	0.78	4.94	4.22	0.47	0.54	1.85	5.87	0.74	0.76	1.13	1.88
Constant (n)	1.2483	1.8208	0.6439	0.8730	0.6857	0.4699	0.3793	0.6279	0.4494	0.4202	0.3316	0.2991	0.4223	0.5469	0.2750	0.3551	0.4321	0.4905
RSD ($\mu g\ kg^{-1}$)	*9.87*		*18.60*		*20.26*		*11.56*		*15.60*		*22.19*		*17.34*		*24.57*		*13.78*	
Inf-exp																		
Constant (n)	4.2156	5.4323	3.3219	4.2523	1.0241	3.1066	0.5759	0.7549	2.7232	2.4484	0.3577	0.3329	0.6787	2.9768	0.3124	0.3994	0.5426	0.7989
RSD ($\mu g\ kg^{-1}$)	*15.84*		*34.34*		*38.61*		*19.20*		*48.64*		*21.40*		*36.63*		*24.38*		*20.53*	
Spherical Diffusion + kd																		
kd (L kg^{-1})	0.000	0.000	0.000	0.000	0.000	0.000	0.585	0.000	0.144	0.385	0.329	0.300	0.724	0.079	0.659	0.501	0.270	0.043
D/r^2	0.0847	0.1440	0.0436	0.0741	0.0146	0.0343	0.0054	0.0100	0.0232	0.0160	0.0017	0.0016	0.0062	0.0290	0.0011	0.0020	0.0051	0.0105
RSD ($\mu g\ kg^{-1}$)	*10.31*		*15.33*		*19.19*		*17.86*		*10.02*		*10.44*		*16.97*		*13.42*		*14.29*	

Table 5: Residual standard deviations for the single spherical diffusion model implemented with all soils simultaneously and parameterised from the soil variables: pH, %SOC and %Ox.

Soil variables	**Number of model coefficients**	**RSD (mg kg^{-1})** ($\times 10^{-2}$)
k_O	4	1.98
k_O, k_{pH}	8	1.56
k_O, k_{pH}, k_C	12	1.09
k_{pH}, k_C, k_{ox}	14	0.0850

Table 6: Values of optimised soil coefficients (k_O, k_{pH}, k_C, k_{Ox}) for the single spherical diffusion model implemented with all soils simultaneously and parameterised from the soil variables: pH, %SOC and %Ox.

Soil coefficients	**10°C incubation**		**20°C incubation**	
	kd; Equ. 12	$p(D/r^2)$; Equ. 11	kd; Equ. 12	$p(D/r^2)$; Equ. 11
k_O	0	4.13	0	4.11
k_{pH}	-0.814	-0.0876	-0.878	-0.113
k_C	-38.4	-0.181	-47.4	-0.160
K_{Ox}	419	0.253	478	0.179

FIGURE CAPTIONS

Figure 1: Stacked plots where the total height of the bar represents total ^{129}I in solution after equilibration with 0.01 M KNO_3 at 10°C, with associated error bar. Dark grey bar represents amount present as $^{129}IO_3^-$, again with associated error. The difference between the total ^{129}I and $^{129}IO_3^-$, given by the light grey bar represents the amount of ^{129}I-org in solution.

Figure 2: Stacked plots where the total height of the bar represents total ^{129}I in solution after equilibration with 0.01 M KNO_3 at 10°C, with associated error bar. Dark grey bar represents amount present as $^{129}I^-$, again with associated error. The difference between the total ^{129}I and $^{129}I^-$, given by the light grey bar represents the amount of ^{129}I-org in solution.

Figure 3: Schematic diagram showing proposed reaction paths of iodine in soils.

Figure 4: Modelling kinetics of (a) iodate and (b) iodide ^{129}I sorption: box and whisker plots showing the distribution of residual standard deviations (RSD; μg kg^{-1}) across nine contrasting soils for each of the nine models tested. The mean value (•) and outliers (*) are shown.

Figure 5: Comparison of the measured loss from solution of a 0.15 mg kg^{-1} $^{129}IO_3^-$ spike added to soils and incubated at 10°C and 20°C with model predictions for that soil fitted using a spherical diffusion model with kd (Sph-Diffn+kd)**.**

Figure 6: Comparison of the measured loss from solution of a 0.15 mg kg^{-1} $^{129}I^-$ spike added to soils and incubated at 10°C and 20°C with model predictions for that soil fitted using a spherical diffusion model with kd (Sph-Diffn+kd).

Figure 7: Iodate concentration in solution (mg kg^{-1} soil) modelled for all soils incubated at 10°C with a spherical diffusion model (Equation 8, Table 2). Model parameters ($p(D/r^2)$ and kd) were estimated from the soil variables

pH, %SOC and %Ox (Equations 11 and 12). The solid line as a 1:1 relation and the dashed lines represent a displacement of one residual standard deviation (RSD).

Figure 8: Apparent activation energies (Ea, kJ mol^{-1}) from spherical diffusion model as a function of soil organic carbon content (%); solid line represents the average value.

Figure 9: Simulation of iodate sorption as a function of % soil organic carbon (SOC), pH and temperature using the parameterised spherical diffusion model. The proportion of iodate remaining in solution is shown for a hypothetical soil with 5% $Fe(OH)_3$ and 1% MnO_2 at pH 4 or 7 and at a temperature of 10^{o}C or 20^{o}C.

Figure 10: Mole ratio (x 10^{-6}) of iodine to organic carbon as a function of depth in woodland (△) and arable (○) soil profiles from the Sutton Bonington site; solid lines are logarithmic fits – i.e. ln(ratio)=(depth-k1)/k2.

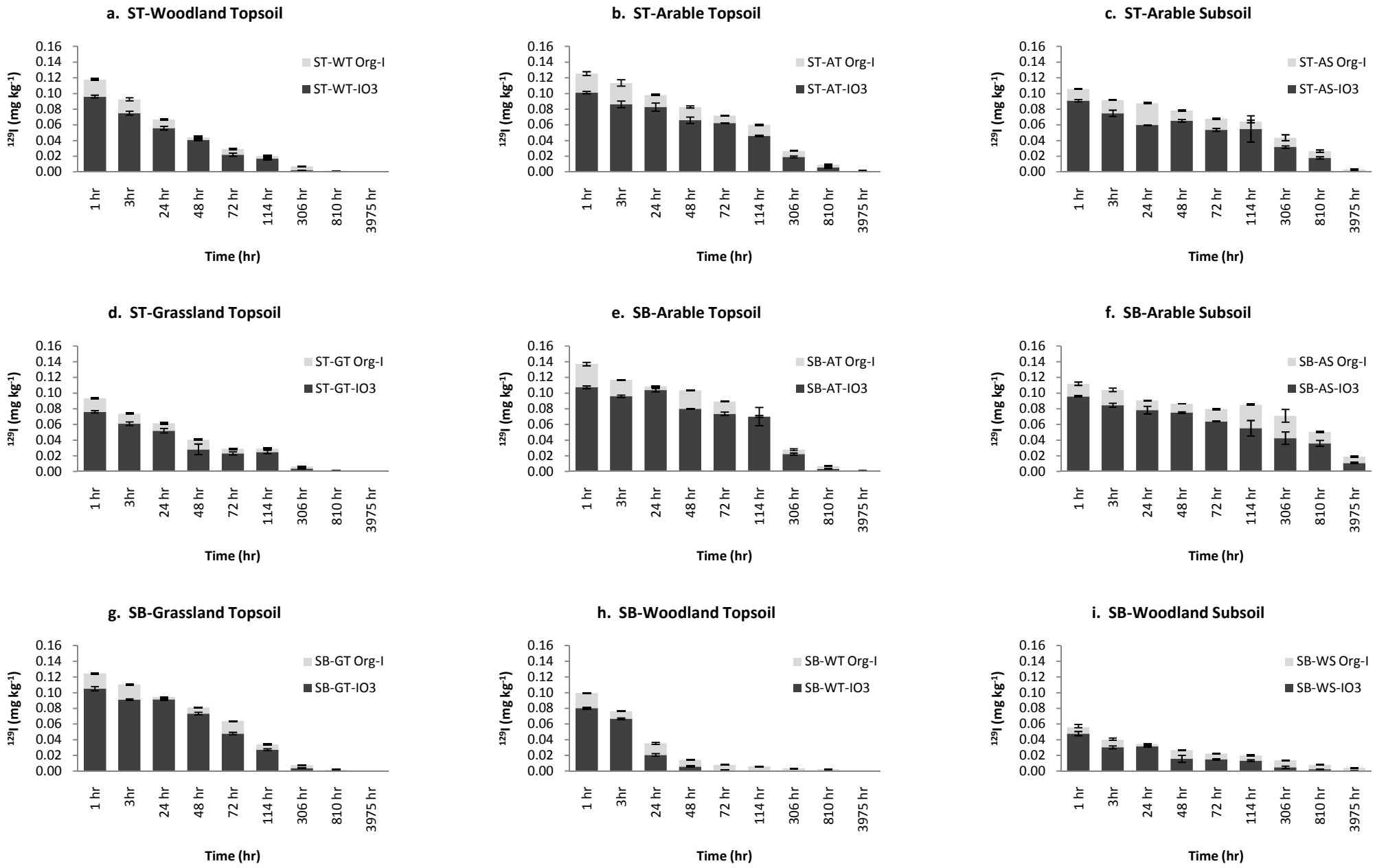
a. ST-Woodland Topsoil
b. ST-Arable Topsoil
c. ST-Arable Subsoil
d. ST-Grassland Topsoil
e. SB-Arable Topsoil
f. SB-Arable Subsoil
g. SB-Grassland Topsoil
h. SB-Woodland Topsoil
i. SB-Woodland Subsoil
129I (mg kg-1)
0.16
0.14
0.12
0.10
0.08
0.06
0.04
0.02
0.00
ST-WT Org-I
ST-WT-IO3
ST-AT Org-I
ST-AT-IO3
ST-AS Org-I
ST-AS-IO3
ST-GT Org-I
ST-GT-IO3
SB-AT Org-I
SB-AT-IO3
SB-AS Org-I
SB-AS-IO3
SB-GT Org-I
SB-GT-IO3
SB-WT Org-I
SB-WT-IO3
SB-WS Org-I
SB-WS-IO3
1 hr
3hr
24 hr
48 hr
72 hr
114 hr
306 hr
810 hr
3975 hr
Time (hr)

Figure 1

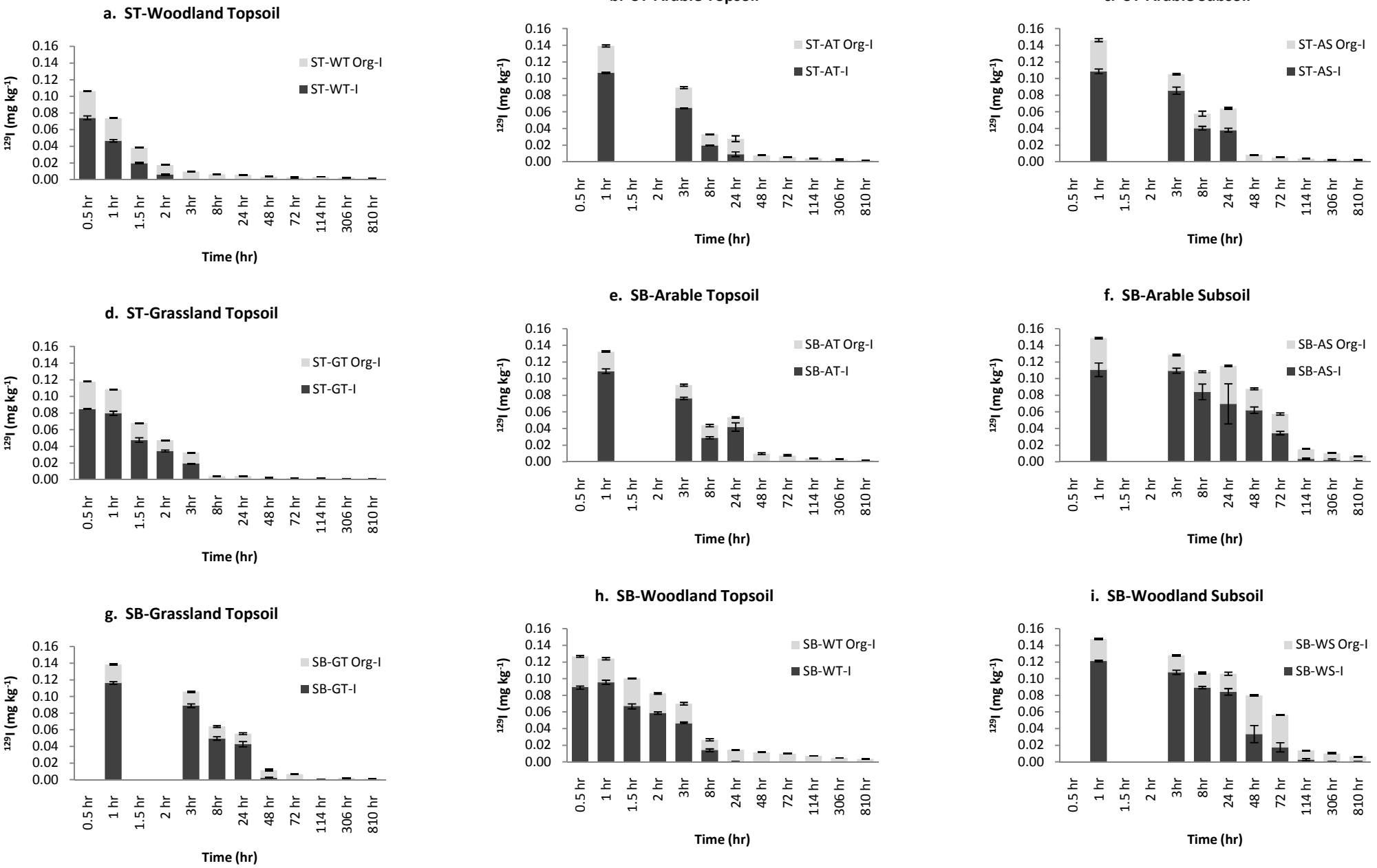
a. ST-Woodland Topsoil
ST-WT Org-I
ST-WT-I
b. ST-Arable Topsoil
ST-AT Org-I
ST-AT-I
c. ST-Arable Subsoil
ST-AS Org-I
ST-AS-I
d. ST-Grassland Topsoil
ST-GT Org-I
ST-GT-I
e. SB-Arable Topsoil
SB-AT Org-I
SB-AT-I
f. SB-Arable Subsoil
SB-AS Org-I
SB-AS-I
g. SB-Grassland Topsoil
SB-GT Org-I
SB-GT-I
h. SB-Woodland Topsoil
SB-WT Org-I
SB-WT-I
i. SB-Woodland Subsoil
SB-WS Org-I
SB-WS-I
129I (mg kg-1)
0.00
0.02
0.04
0.06
0.08
0.10
0.12
0.14
0.16
0.5 hr
1 hr
1.5 hr
2 hr
3hr
8hr
24 hr
48 hr
72 hr
114 hr
306 hr
810 hr
Time (hr)

Figure 2

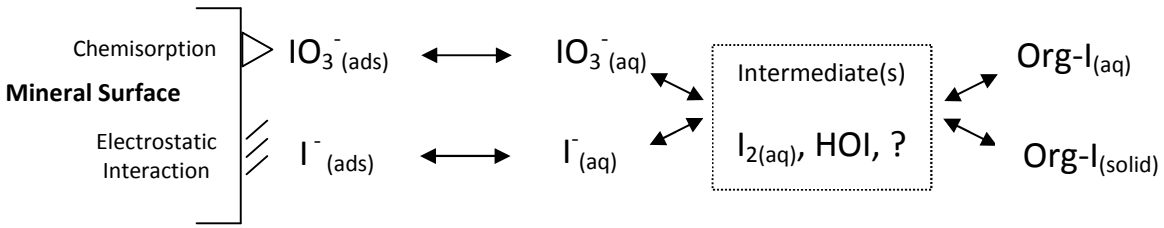
Chemisorption
Mineral Surface
Electrostatic Interaction
IO_3^- (ads)
I^- (ads)
IO_3^- (aq)
I^- (aq)
Intermediate(s)
$I_{2(aq)}$, HOI, ?
Org-$I_{(aq)}$
Org-$I_{(solid)}$

Figure 3

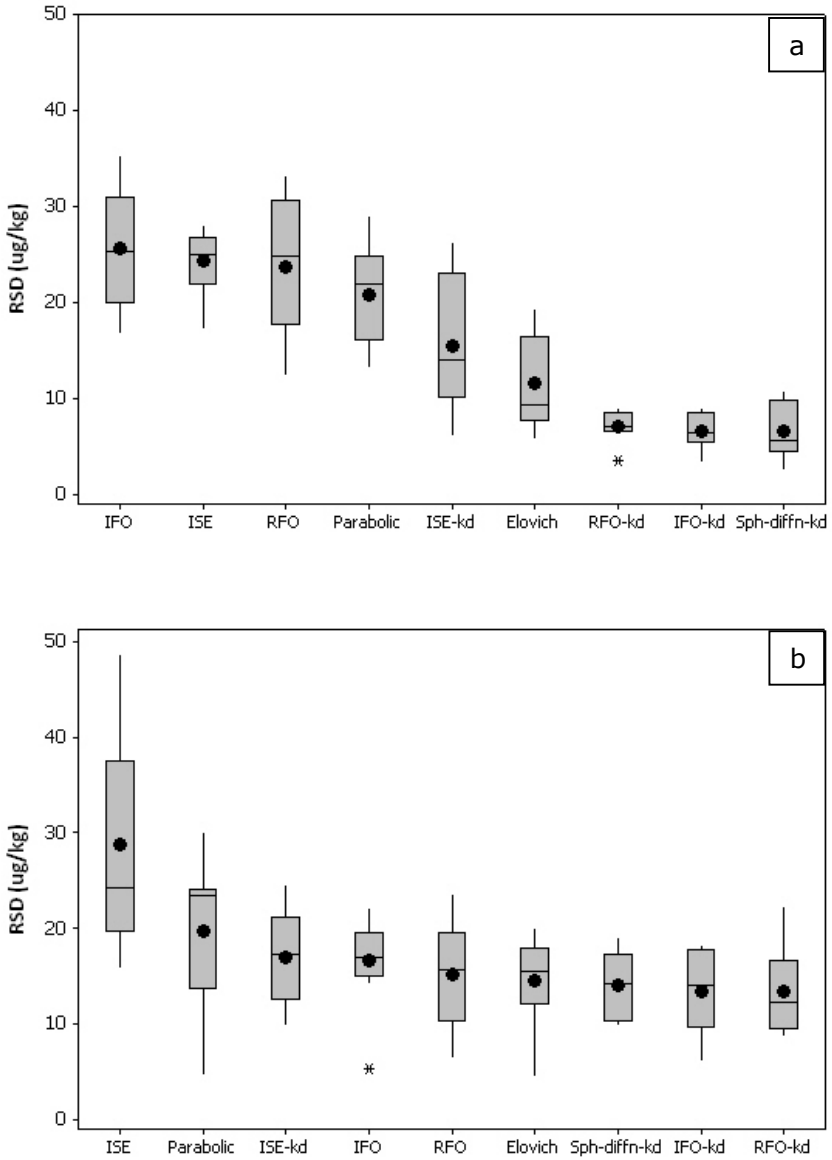
a
RSD (ug/kg)
50
40
30
20
10
0
IFO
ISE
RFO
Parabolic
ISE-kd
Elovich
RFO-kd
IFO-kd
Sph-diffn-kd
b
RSD (ug/kg)
50
40
30
20
10
0
ISE
Parabolic
ISE-kd
IFO
RFO
Elovich
Sph-diffn-kd
IFO-kd
RFO-kd

Figure 4

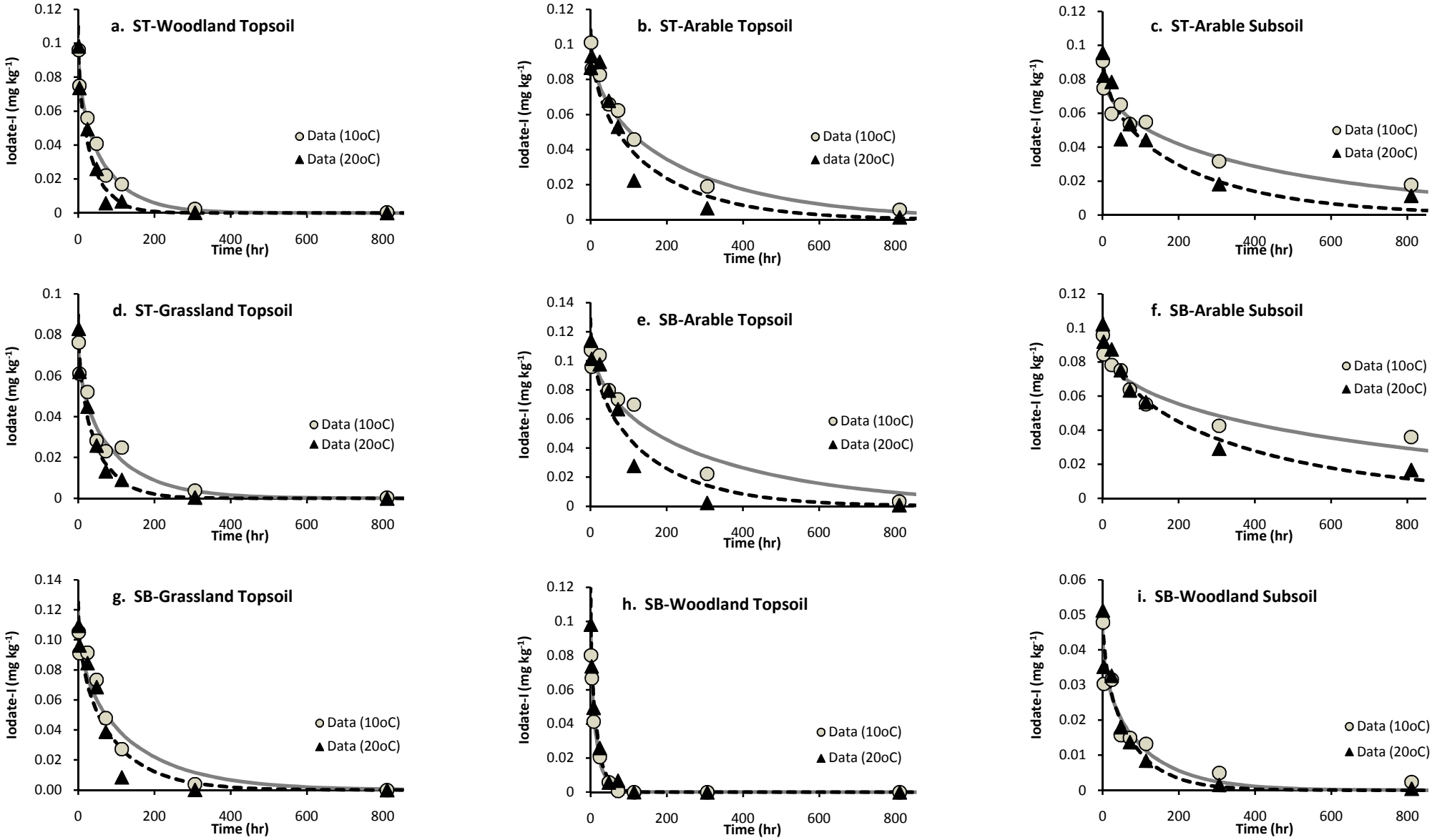
a. ST-Woodland Topsoil
b. ST-Arable Topsoil
c. ST-Arable Subsoil
d. ST-Grassland Topsoil
e. SB-Arable Topsoil
f. SB-Arable Subsoil
g. SB-Grassland Topsoil
h. SB-Woodland Topsoil
i. SB-Woodland Subsoil
Iodate-I (mg kg-1)
Time (hr)
Data (10oC)
Data (20oC)
data (20oC)

Figure 5

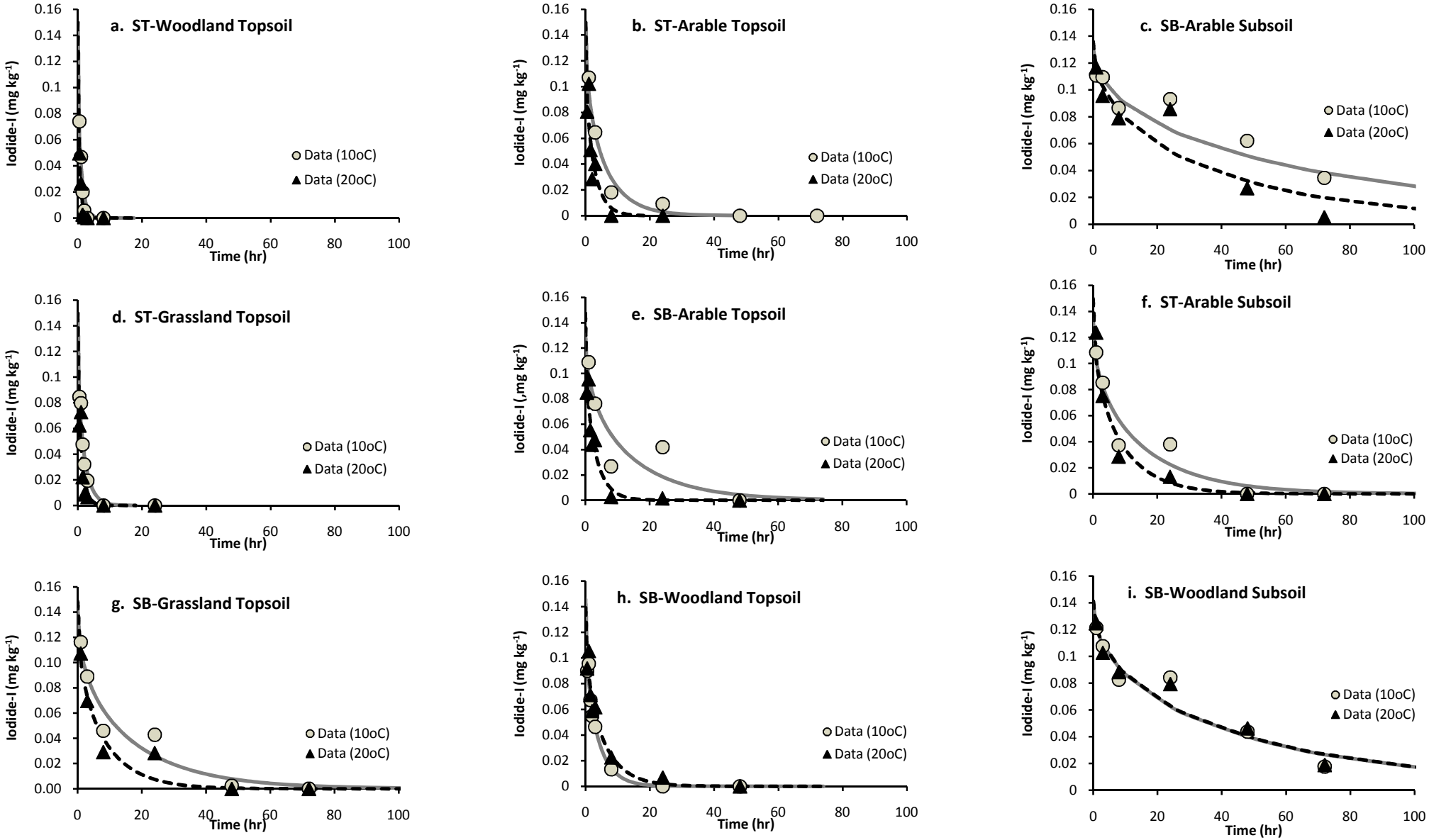
a. ST-Woodland Topsoil
b. ST-Arable Topsoil
c. SB-Arable Subsoil
d. ST-Grassland Topsoil
e. SB-Arable Topsoil
f. ST-Arable Subsoil
g. SB-Grassland Topsoil
h. SB-Woodland Topsoil
i. SB-Woodland Subsoil
Iodide-I (mg kg-1)
Time (hr)
Data (10oC)
Data (20oC)

Figure 6

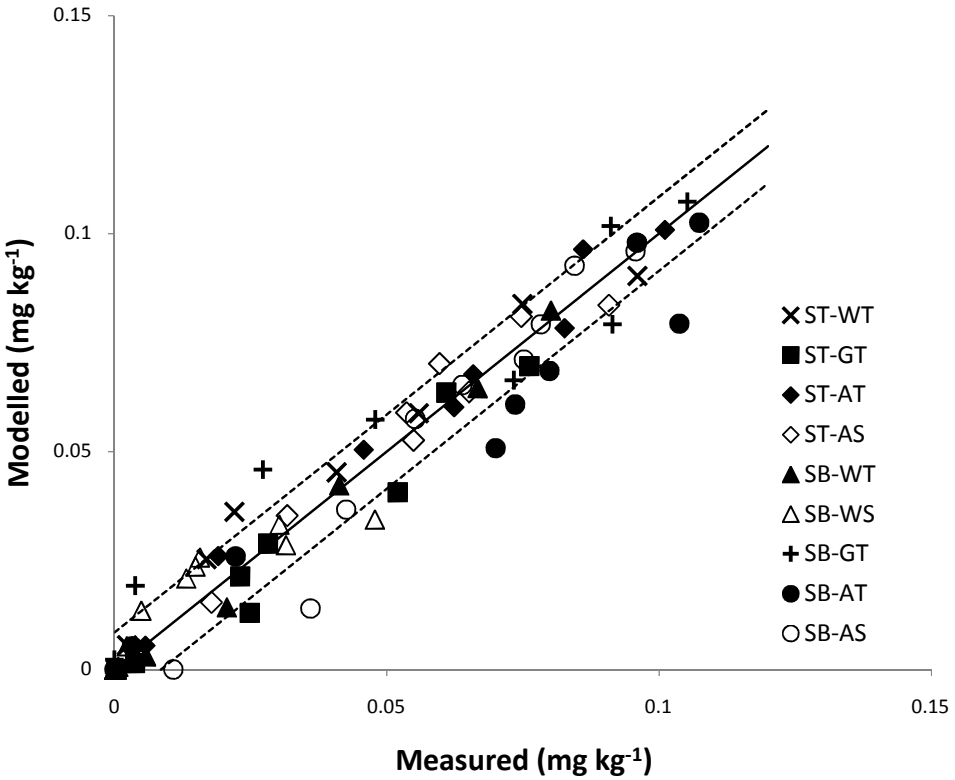
0.15
0.1
0.05
0
Modelled (mg kg-1)
0
0.05
0.1
0.15
Measured (mg kg-1)
ST-WT
ST-GT
ST-AT
ST-AS
SB-WT
SB-WS
SB-GT
SB-AT
SB-AS

Figure 7

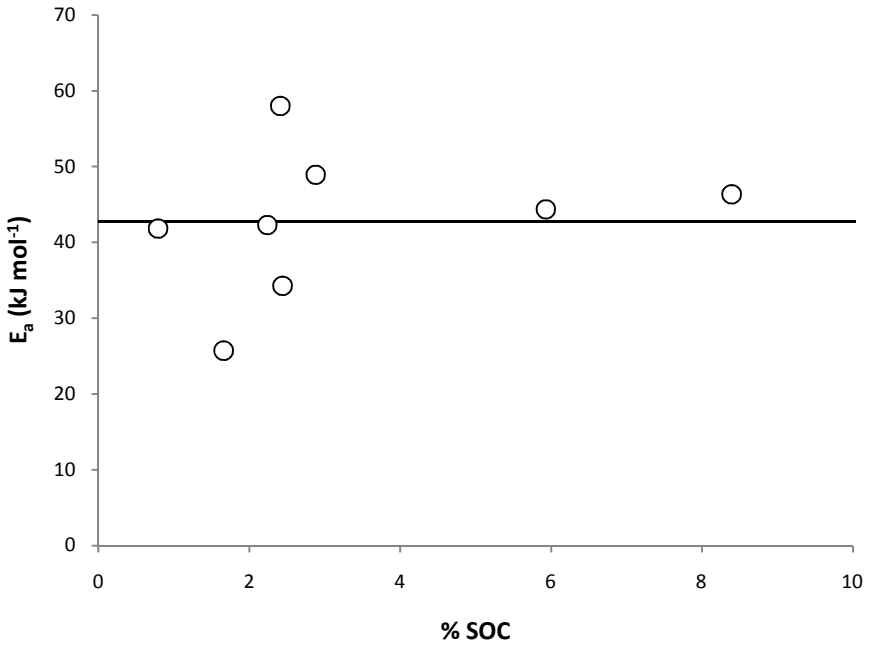

Figure 8

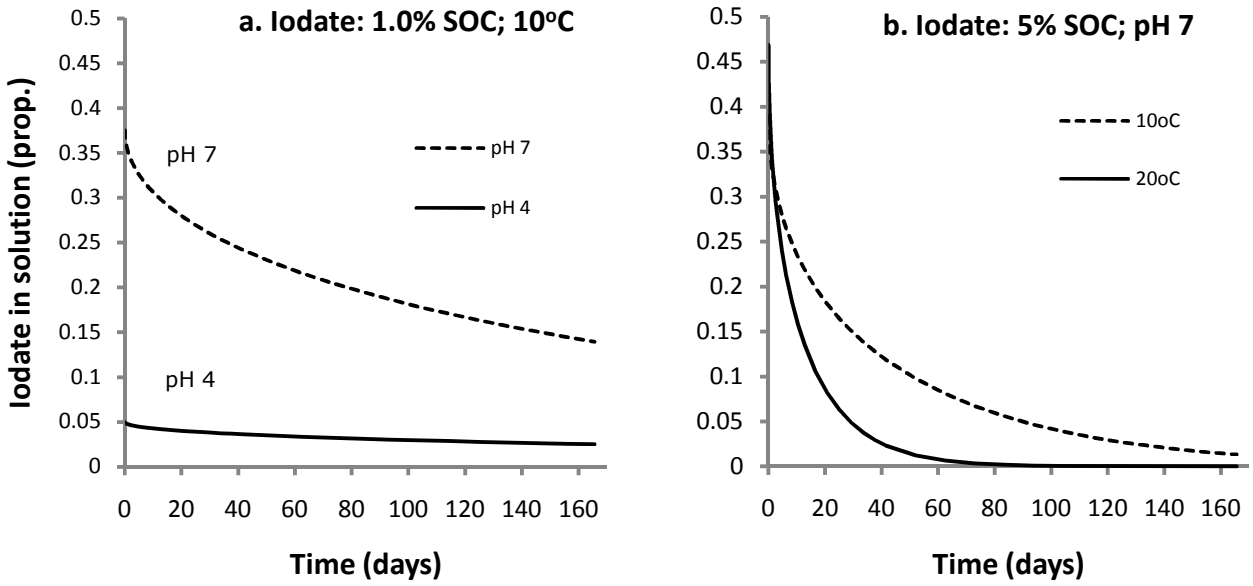
a. Iodate: 1.0% SOC; 10oC
Iodate in solution (prop.)
0.5
0.45
0.4
0.35
0.3
0.25
0.2
0.15
0.1
0.05
0
pH 7
pH 4
0 20 40 60 80 100 120 140 160
Time (days)
b. Iodate: 5% SOC; pH 7
10oC
20oC
Time (days)

Figure 9

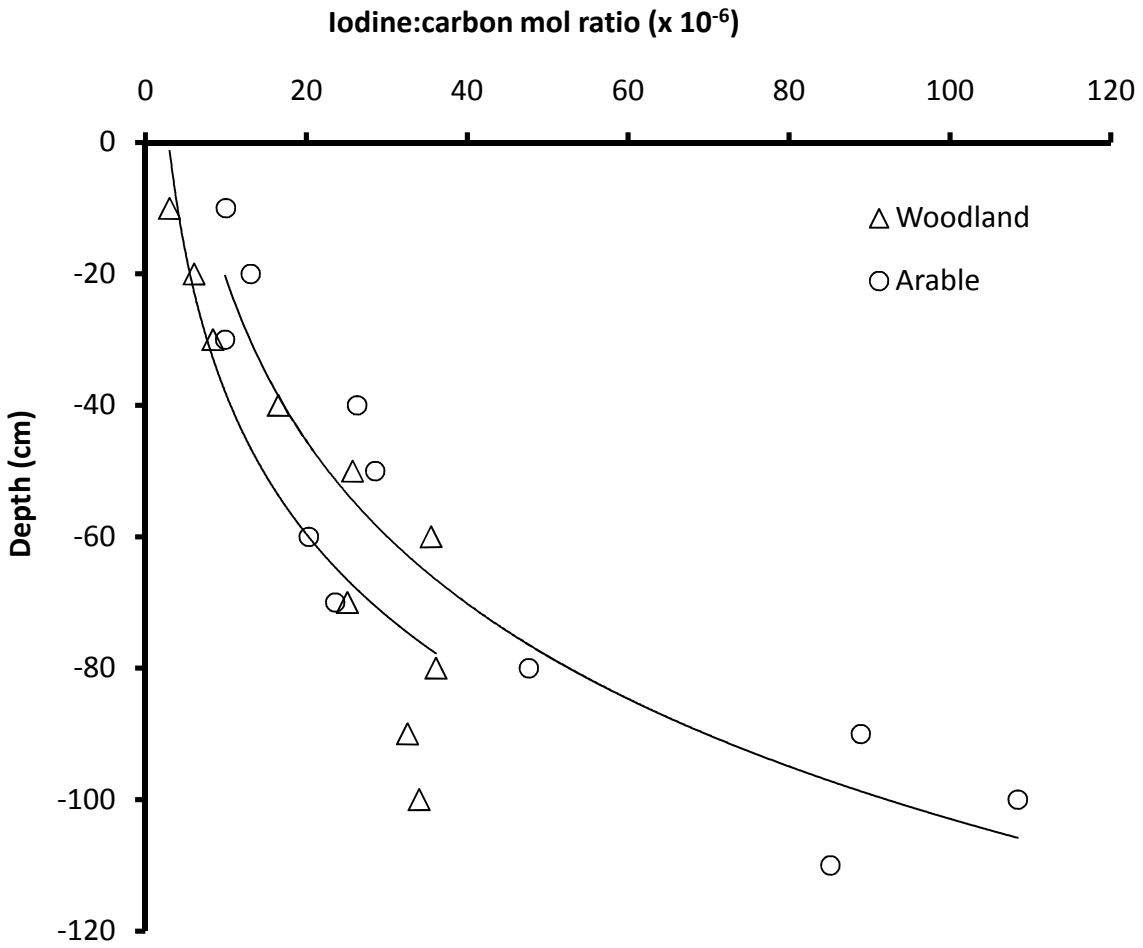
Iodine:carbon mol ratio (x 10-6)
0
20
40
60
80
100
120
0
-20
-40
-60
-80
-100
-120
Depth (cm)
Woodland
Arable

Figure 10